Title

An expanding human footprint drives escalating human—elephant conflict across a transboundary African landscape through 2085

Journal

PNAS Nexus, 5(7)

ISSN

2752-6542

Authors

Patrick, Evan

Pepperdine, Maxwell

Yu, Christy

et al.

Publication Date

2026-06-29

DOI

10.1093/pnasnexus/pgag205

PNAS nexus

Main Manuscript for

An expanding human footprint drives escalating human-elephant conflict across a transboundary African landscape through 2085

E. Patrick[1], M. Pepperdine[1], C. Yu[1], S. Pesek[2], O. Somhegyi[3], J. Krieger[4], N. McManus[4], E. Fabiano[5], C. Sikopo[6], P. Roehrdanz[4], A. Larsen[1]

Author Affiliations

[1]Bren School of Environmental Science & Management, University of California, Santa Barbara, 93106-5131, USA. [2]Energy and Resources Group, University of California, Berkeley, 345 Giannini Hall, Berkeley, CA 94720, USA. [3]Conservation Biology Institute, 136 SW Washington Ave., Corvallis, OR 97333, USA. [4]The Moore Center for Science and Solutions, Conservation International, 2011 Crystal Dr., Arlington, VA, 22202, USA. [5]Department of Wildlife Management and Tourism Studies, University of Namibia, Katima Mulilo 1096, Namibia. [6]Ministry of Environment, Forestry and Tourism, Windhoek 13306, Namibia

Corresponding author: Dr. Evan Patrick
Email: epatrick@ucsb.edu

Competing Interest Statement: Evan Patrick has a consulting relationship with Carbon Direct Inc., a company combining science, technology, and capital to deliver quality carbon dioxide management at scale.

Classification

Major: Biological, Health, and Medical Sciences
Minor: Environmental Sciences

Keywords

Human-wildlife conflict; land use change; biodiversity; causal inference; species distribution modeling

This PDF file includes:

Abstract

Rapid land-use change is compressing the space between people and wildlife at an unprecedented pace, elevating concerns of conflict between people and keystone megafauna such as the African savanna elephant (*Loxodonta africana*). However, the underlying drivers of human-elephant conflict (HEC) are often inferred but not causally identified, and forecasting under future scenarios is limited, restricting our ability to anticipate where and why conflict will intensify. Using a dataset on conflict events from 2004 to 2020 across a transboundary landscape in Southern Africa, we integrate causal inference (panel data regressions) and machine learning (point process models) to link mechanisms with spatial forecasts. We find that human population growth, cropland expansion, and climate-driven aridity in core elephant protected areas drive conflict risk. Furthermore, we show that landscape features such as wildlife fences and roads constrain elephant movement in ways that drive HEC. Applying these models to projected land use, population, and climate under future coupled climate-development scenarios, we find that the area at high risk of HEC increases by 33% to 100% by 2085 with corresponding rises in event frequency. Aggressive human land-use expansion leads to the most dramatic increases in conflict, with climate impacts playing a significant but smaller role. These results identify emerging conflict hotspots decades in advance, offering actionable foresight for land use planning and mitigation in a region critical to elephant conservation.

Significance

Human-wildlife conflict is accelerating globally as agriculture and settlements expand into wildlife ranges, yet planners lack spatially explicit tools to anticipate where conflict will intensify. Using a multi-model approach, we identify the drivers and spatial patterns of historic and future elephant crop raiding across Africa's largest transboundary conservation landscape. We find human land use and population expansion primarily drive conflict rates, outweighing impacts from climate, and pinpoint locations where conflict risk will intensify decades in advance, providing an unprecedented window for intervention. By combining two complementary forecasting methods, we create a more complete picture of potential shifts in the patterns of human-wildlife conflict, offering a framework for researchers to assess conflict risk and future change in transfrontier landscapes globally.

1 Introduction

Global environmental change is reshaping interactions between people and wildlife. Expansion of agriculture, settlements, and infrastructure is increasing the frequency of encounters, while climate-driven shifts in water and forage availability can redirect animal movement toward human resources and amplify conflict (Abrahms et al., 2023). Recent global analyses project that human-wildlife overlap will expand across more than half of terrestrial land area by 2070 (Ma et al., 2024), heightening the need for spatially explicit tools that can anticipate emerging conflict hotspots and identify actionable drivers.

Southern Africa is home to most of the world's remaining savanna elephants (*Loxodonta africana*), with many populations stabilizing or even rebounding in recent decades (Huang et al., 2024). At the same time, the region's human population is growing at around 2.5% annually (Stoldt et al., 2020), leading to the expansion of human settlements and agriculture and increasing spillovers of elephants into human-dominated landscapes. Resulting human-elephant conflict (HEC), including crop raiding, injury to people, or destruction of infrastructure and livestock, is often devastating for impacted households and can erode community support of conservation (Mwangi et al., 2016; Nsonsi et al., 2018). In extreme cases, this leads to the culling of elephants (Shaffer et al., 2019), underscoring a consequential misalignment between conservation priorities and human livelihood policies. These trends, alongside the potential of growing climate pressures to further escalate conflict (Abrahms, 2021), present critical challenges for resource managers in the region.

These conservation challenges intersect directly with the socioeconomic realities of affected communities. In Namibia, elephant crop raiding, the most common form of HEC, can result in economic damages that outweigh local benefits from trophy hunting (Drake et al., 2021). Given its clear relevance to conservation and livelihoods, many studies have examined the drivers and distribution of HEC (Branco et al., 2019; Jayakody et al., 2024; Munyao et al., 2020; Thant et al., 2021). However, most of these studies do not consider global change pathways that could substantially alter elephant movement, population health, and conflict

prevalence in the future (Dejene et al., 2021; Guarnieri et al., 2024). While past work has shown overlap between human dominated landscapes and elephant ranges under varying climate scenarios (Guarnieri et al., 2024), and climate is recognized as a conflict amplifier (Abrahms et al., 2023), there remains a critical need to map the drivers, prevalence, and extent of HEC into the future.

Previous research on HEC has generally used one of two approaches based on disciplinary focus: either causal inference statistical methods or machine learning models. Causal inference methods, common in economics, political science and public health, identify specific drivers of HEC, such as settlement density (Graham et al., 2010) or cropping patterns (Mukeka et al., 2019). These methods help describe the mechanisms that give rise to HEC, though they are sometimes challenged by complex, non-linear and dynamic ecological relationships. Alternatively, a growing body of HEC research applies methods derived from machine learning to understand the patterns and distribution of HEC (Naha et al., 2019; Rani et al., 2024), providing explicit maps of conflict hotspots with generally higher predictive power than regression methods, though with less focus on mechanisms or causality. In our analysis, we integrate these complementary approaches, leveraging the causal identification strengths of econometric methods and the spatial predictive power of machine learning to assess underlying causal drivers and spatial hotspots of HEC now and under future scenarios.

Using a database that tracked incidents of human wildlife conflict, including HEC, from 2004-2020 across Namibia's communal conservancies (community-managed reserves that support tourism and sustainable resource use), we analyzed the drivers and spatial distribution of elephant crop raiding across a transboundary landscape spanning northern Namibia, much of northern Botswana, and portions of Angola and Zambia (Figure 1), hereafter referred to as the study area. We then projected both models forward under multiple coupled climate-development scenarios (SSP-RCPs) to produce the first spatially explicit estimates of changes in the frequency and extent of HEC through 2085. This integration of causal and machine learning approaches allowed us to ask the following questions: 1) What are the current drivers of HEC in the study area? 2) What are the predicted spatial hotspots of HEC events across our study area?

And 3) How will the spatial extent and frequency of HEC change under divergent climate and development pathways? In answering these questions, we provide key insights to guide proactive HEC management in the decades ahead.

2 Method

2.1 Study Area

The study area spans northern Namibia, much of northern Botswana, and portions of Angola and Zambia, encompassing Namibian communal conservancies where HEC was recorded and the surrounding landscapes used by elephants (Figure 1). Elephant populations extend across the north of the study area, with the largest population spanning the transfrontier region of northeast Namibia and adjacent countries (Huang et al., 2022), a population within the fully-fenced Etosha National Park, and a smaller desert-adapted population in Namibia's northwestern highlands (Craig et al., 2021). HEC is most prevalent in the far eastern Zambezi Region and the northwestern highlands, where elephant ranges overlap or border rural human settlements. The Zambezi Region, located within Namibia's eastern panhandle, stands out within Namibia as being relatively wet and amenable to farming, leading to a higher human population density and agricultural footprint than the rest of the country (O'Connell-Rodwell et al., 2000). It also serves as a functional corridor between core elephant reserves such as Chobe and Sioma Ngwezi National Parks (Huang et al., 2022). Namibia's northwestern highlands experience low, variable rainfall and erosive soil, leading to heterogeneous resource availability and highly mobile resource searching behavior in elephants (Wenborn et al., 2025).

We focused on HEC events recorded within Namibia's communal conservancies, but our study area considered the broader landscapes surrounding these conservancies in evaluating the drivers and distribution of HEC. Communal conservancies are self-governing, communal land management organizations formed to gain common property rights over wildlife and tourism operations on local lands (Jones, 2010). While they utilize land-use restrictions to promote conservation, subsistence farming remains a key livelihood strategy for residents.

2.2 Panel Data Regressions

We used two-way fixed effects regression models to identify causal effects of land use and climate variables on HEC. By including fixed effects for spatial groups (500 k-nearest neighbors) and season-years, we exploit within-group temporal variation while removing time-invariant unobserved heterogeneity that could bias estimates in complex ecological systems. This approach differences out unobserved characteristics at the spatial group level and accounts for temporal shocks affecting all conservancies. We verified that our treatment variables, including weather, population, and land use, retained sufficient within-group variation (>10%) for identification (Greene, 2008). While retaining 10% of the total variation within each group, we spatially define 500 k-nearest neighbor groups to control for variation across the landscape, and season-year groups to control for variation across time. Standard errors were clustered at both the spatial group and season-year levels following (Cameron et al., 2011). The model specification is:

$$CropRaid_{igsy} = \beta\, X_{igsy} + \alpha_g + \gamma_{sy} + \epsilon_{igsy} \qquad (1)$$

Where $CropRaid_{igsy}$ represents the number of crop raiding events at grid cell *i*, within spatial group *g*, in season-year *sy*. X_{igsy} is a vector of time-varying covariates (population, land cover, and climate variables) with coefficient vector β. α_g denotes spatial group fixed effects (based on 500 k-nearest neighbors), γ_{sy} represents season-year fixed effects, and ϵ_{igsy} is the error term. Summary statistics of the range and mean values of the events are provided in Table S1.

Finally, because conflict data were provided in count form, we ran negative binomial and Poisson fixed effects regressions to ensure that our linear specification was not over-estimating certain results. These models are discussed in Text S1 and results are presented in Table S2 and Table S3.

2.3 Point Process Model

A point process modeling approach was used to predict the probability of HEC across the study area as a function of key predictor variables. Point process models are commonly used in species distribution modeling to predict distribution based on presence-only records and environmental predictor variables (Phillips et al., 2017). While frequently applied to species occurrence distribution, point process models have also been employed to model the occurrence distribution of HEC (Jayakody et al., 2024; Naha et al., 2019; Rani et al., 2024). We generated two discrete point process models to separately explore patterns and changes in crop raiding during the wet versus the dry season. Occurrences were split by wet/dry season due to strong previously documented patterns and seasonality of HEC (Graham et al., 2010; Mukeka et al., 2019; Munyao et al., 2020). For each model, the final output was a probability distribution across the study area defined by a bounding box encompassing all HEC-reporting Namibian communal conservancies (Figure S1). This is the same extent shown in Figure 1.

While known absences are desired in species distribution and ecological niche modeling, this data is often unavailable (Merow et al., 2013). To account for this within each season, background pseudo-absence points were randomly generated using the `dismo` R package (version 1.3.14). These points were temporally distributed proportional to the number of HEC occurrences in each season-year (e.g., wet season-2004) and within conservancy boundaries, during years in which HEC was reported (Table S5). We aggregated incidents of HEC at each grid cell for each wet and dry season annually between 2004 and 2020, from which we then extracted the conditions of environmental predictor variables to train the point process models.

Sixteen environmental predictor variables were selected based on their ecological importance to model HEC risk (Graham et al., 2010; Jayakody et al., 2024; Naha et al., 2019; Rani et al., 2024): percent land cover (built, cropland, grassland, shrub, tree, water), distance to protected areas, distance to rivers, distance to roads, distance to fences, population density, EVI, SPEI, elevation, slope, and aspect. We tested for variable correlation using Pearson's correlation coefficient (Figure S3) as per (Nettleton, 2014).

We used the `ENMeval` R package (version 2.0.4) to generate and evaluate a series of point process models before selecting the 'best' performing model. Two feature class combinations, linear (L) and linear + quadratic (LQ), were used, with regularization multiplier values ranging from 0.5 to 3 in increments of 0.5, to generate a total of 12 models. More complex feature classes (product, hinge, and threshold) were excluded to avoid overfitting and because these relationships are not easily justified given known elephant movement ecology (Merow et al., 2013, 2014). Spatial block (4-fold) cross-validation was used to partition the data for training and testing during model evaluation to control for spatial autocorrelation (Merow et al., 2014). A discussion of model performance evaluation is provided in Text S2. After selecting the best-performing model, the Jackknife test was used to evaluate the relative importance of each explanatory variable in predicting HEC when generating the final wet and dry season point process models.

2.4 Future Projections

After fitting regressions and the point process model to historical data, we applied both to future projections of climate, land use, and population under multiple scenarios to estimate potential future rates and distributions of HEC. For temperature, precipitation, land cover, and population, we calculated changes from a baseline (2011-2040 climatology for climate data; 2025 for land cover and population) to projected periods (2041-2070 / 2055 and 2071-2100 / 2085). Regression projections used the delta method to estimate standard errors, applying the same covariate structure as the fitted models (Fox et al., 2012; Oehlert, 1992). The best-performing point process model was rerun with future data to predict HEC distribution across the study area for 2025, 2055, and 2085 under four scenarios (SSP1-RCP2.6, SSP2-RCP4.5, SSP3-RCP7.0, SSP5-RCP8.5), following best practices for species distribution modeling (Merow et al., 2013). Continuous point process model outputs were converted to binary presence/absence using the threshold (0.72) that maximized Cohen's Kappa for the point process model, and changes were mapped by subtracting the 2025 binary raster from 2055 and 2085 predictions. Thresholding enables the creation of simple, easily interpretable maps (Merow et al., 2013) to compare predicted hotspots in point process modeling.

2.5 Human-Elephant Conflict Data

We obtained monthly HEC data for 2004-2020 from the Conservation Information (ConInfo) database managed by the Natural Resources Working Group of the Namibian Association of Community Based Natural Resource Management. Events were self-reported by farmers and verified by audits as part of a compensation payment program (MEFT & NACSO, 2022). Data were recorded in a 2 km grid (Figure S6) that serves as our unit of analysis (hereafter referred to as the 'HEC grid'). We focused on crop raiding events, which constituted over 90% of the conflict events in the dataset. As crop raiding is likely influenced by seasonal changes in vegetation productivity (Branco et al., 2019; Loarie et al., 2009), events were aggregated by wet (November-April) and dry (May-October) seasons. May events were included in the wet season to account for crop harvesting that extends into the early dry season.

2.6 Landscape Characteristics

At the landscape level, we compiled datasets describing human landscape use, features that elephants preferentially use, and features that may hinder elephant movement. All datasets were resampled to match the resolution of the HEC grid using mean aggregation, unless otherwise specified. Since roads can act as either barriers or corridors for elephant movement and are associated with HEC events (Naha et al., 2019), we included distance to roads as a predictor variable, using road data from OpenStreetMap (Haklay & Weber, 2008). We pulled yearly human population counts from WorldPop (WorldPop, & Bondarenko, 2020), as population is a well-documented predictor of HEC (Graham et al., 2010; Mukeka et al., 2019; Munyao et al., 2020). Human and natural land cover (built-up area, cropland, shrub cover, grassland cover, tree cover, and water) were tracked from 2004 to 2020 using the Copernicus Climate Change Initiative (CCI) Global Plant Functional Type dataset (Harper et al., 2023). Because elephants often track anomalously green patches across the landscape (Loarie et al., 2009), we used the Enhanced Vegetation Index (EVI) from the global MODIS vegetation indices V061 averaged across season-year (Didan, 2021). Water sources are also important preferential features for elephant movement (Tsalyuk et al., 2019); therefore, we used global rivers data

from HydroRIVERS, filtered to rivers with catchment areas of at least 10 km² or an average river flow of at least 0.1 m³/s, or both (Lehner & Grill, 2013), and calculated distance to the nearest river. Veterinary fences, which can shift conflict by concentrating elephant movement (Smith & Kasiki, 2000), were taken from Huang et al. (2022) to calculate distance to the nearest fence. Elevation and slope were derived from US Geological Survey (2010) to characterize topographic variability. Finally, to assess connectivity from HEC grid cells to elephant population centers, we used elephant core areas defined by Huang et al. (2024) sourced from Protected Planet (UNEP-WCMC, 2024) and calculated distance to the nearest core area.

2.7 Historical Climate Data

For 2004-2020, we extracted monthly precipitation and mean temperature from the CHELSA dataset (Karger et al., 2017), resampled to the 2 km conflict grid using mean aggregation, and used these to calculate the 3-month Standardized Precipitation Evapotranspiration Index (SPEI). When CHELSA data were unavailable (mainly after June 2019), we used ERA5 surface temperature and summed precipitation (Hersbach et al., 2020), resampled to the HEC grid using nearest neighbors. We selected the 3-month SPEI as it captures seasonal changes in water availability while reflecting vegetation-level water stress (Homdee et al., 2016). SPEI values were also computed for elephant core areas and for a 50 km buffer around each HEC grid cell to assess landscape-scale water availability.

2.8 Global Change Datasets

To project future HEC dynamics, we extracted 3-month SPEI from the Global Drought Layers dataset, which provides 0.25° projected drought indices from 1980-2100 based on downscaled Climate Model Intercomparison Project Phase 6 (CMIP6) models across shared socioeconomic pathways (SSPs; Araujo et al., 2025). We used the five models identified in the Intersectoral Impact Model Intercomparison Project (ISIMIP) as per (Karger et al., 2017) and calculated mean wet- and dry-season 3-month SPEI under representative concentration pathway (RCP) 2.6, RCP4.5, RCP7.0, and RCP8.5 for 2041-2070 and 2071-2100. These values represent the average SPEI departure across models from the 1980-2015 historical baseline to 2055 and 2085, the midpoints of these 30-year ranges.

Future land cover was taken from global projections by (Chen et al., 2022), which provide 1 km resolution classifications every five years for 2015-2100 under each coupled SSP-RCP scenario. We extracted the same cover types used in the historical CCI dataset and converted categorical data to percentage cover at the HEC grid resolution, producing coarse percentage estimates roughly consistent with the historical baseline. Human population density for 2025, 2055, and 2085 was obtained from the FPOP dataset (Li et al., 2022), which provides 1 km global projections for SSPs 1-5 from 2020-2100. These were used to calculate population change at the HEC grid level.

3 Results

3.1 Drivers of Human-Elephant Conflict

We found that rising human population and increases in cropland and built-up cover led to higher levels of crop raiding, all else being equal. Population increases within fixed effects groups were a significant predictor of crop raiding across seasons (Table 1), while increases in cropland and built area were associated with higher wet season conflict. We found that drier core elephant protected areas, as measured through 3-month SPEI, were predictive of higher wet season conflict in nearby conservancies, suggesting a spillover effect from variable habitat suitability in reserves. While this climate driver was significant, variation in human population and land cover were overall more predictive of crop raiding conflict over our study period.

As event data often do not follow a normal distribution as required for unbiased linear models, we also ran Poisson and negative binomial regressions which are tailored to the distributions expected from zero-bounded count data. These regressions produced similar results, confirming the robustness of anthropogenic predictors to count model specifications (Table S2 and Table S3). We also estimated random effects models to incorporate time-invariant landscape characteristics into our prediction of HEC events. While Hausman tests indicated fixed effects specifications were preferred for wet season crop raiding ($p < 0.05$), we found that areas closer to fences and farther from roads were more likely to experience conflict, suggesting that these features constrain elephant movement and drive HEC patterns (Table S4).

3.2 Predicted Conflict Hotspots

Using a point process modeling approach, we generated predictions of continuous HEC probability throughout the study area (Figure 1) as a function of key environmental predictor variables. During the wet season, predicted crop raiding hotspots are concentrated along the northern boundary of Etosha National Park in northwest Namibia (Figure 2b) and across the Zambezi Region in the northeast (Figure 2c). Additional high-risk areas include the western section of Namibia's panhandle in the Kavango East Region and areas north of Khaudum National Park. In northern Botswana, much of the region included in the study area was also identified as a HEC hotspot, particularly regions along the Okavango Delta and near the Moremi Wildlife Reserve. Predictions of crop raiding during the dry season were broadly similar to those observed in the wet season (Figure S2). Jackknife analyses of the point process models indicate that regularized training gains declined most when tree cover, distance to roads, distance to fences, population, and distance to rivers were excluded (Figure S5), implying that these variables best contributed to the collective model's HEC predictive capability. Across both seasonal models, EVI and tree cover emerged as the most influential individual predictors of HEC, and distance to rivers and grassland cover contributed moderate predictive power by themselves (Figure S5).

3.3 Future Conflict Projections

We project out estimated changes in conflict from 2025 to 2085 under SSP1-RCP2.6 ("sustainability"), SSP2-RCP4.5 ("middle of the road"), SSP3-RCP7.0 ("regional rivalry") and SSP5-RCP8.5 ("fossil-fueled development") scenarios by applying our panel regressions and point process models to projected data. Regression projections represent the expected change in grid-level conflict per year, whereas point process model projections examine changes in the extent of predicted conflict presence. While the scale of change varied by scenario, all scenarios predicted moderate to large increases in crop raiding events (Table S6). SSP3-RCP7.0 ("regional rivalry") represents a worst-case scenario for HEC, with twice as much wet season crop raiding as seen under the SSP1-RCP2.6 ("sustainability") scenario (Figure 3). While SSP5-RCP8.5 ("fossil-fueled development") saw dramatic climate impacts, it projects less land conversion and

moderate population growth for Namibia and resultantly had relatively lower rates of HEC (Table S6). Our models, therefore, predict the worst HEC increases under more aggressive future expansion of human population and land uses, rather than under the most severe climate disruption.

The point process models predict a general increase in the probability of crop raiding HEC toward the end of the century under all emission scenarios in both wet and dry seasons throughout the study area (Figure S10 and Figure S11), aligning with regression-based estimates. Conflict levels were lowest under SSP1-RCP2.6 ("sustainability"), and highest under SSP3-RCP7.0 ("regional rivalry") (Figure 4). Predicted hotspots were similar to the baseline point process model results (Figure 2), with concentrations north of Etosha National Park and along the southwestern boundary of the Zambezi Region in Namibia, and along the periphery of the Okavango Delta and the eastern edge of Moremi Wildlife Reserve in Botswana. Comparisons of areas seeing the most increase in HEC between point process model and regression outputs revealed substantial discrepancies (Figure S12 and Figure S13), likely due to the regressions' spatial fixed effects, which limited projections to within-group deviations and increased sensitivity to population changes. In contrast, point process models incorporated spatial patterns across the full study area, making it more responsive to land cover changes.

4 Discussion

We predict HEC to rise in both frequency and spatial extent under all future scenarios. Both the regression and machine learning approaches consistently project the largest increases under SSP3-RCP7.0, with SSP1-RCP2.6 yielding the lowest conflict levels. When compared with baseline data, these increases represent a trend of increasing overlap and discord between elephants and human populations. Our analysis found that growth of human populations and land uses are the primary drivers of future HEC changes, with climate-driven water deficits potentially influencing the movement of elephants out of core areas and into nearby agricultural areas.

Comparing the outputs of our two modeling approaches highlights their complementarity: regression models identified human-driven changes through within-group variation, while point process models captured fine-scale spatial gradients and unimodal relationships. Furthermore, the random effects regressions (Table S4) and point process models (Figure S5) similarly find that human landscape features like roads and wildlife fences predict HEC risk. When considered together, these models suggest that HEC emerges from both dynamic anthropogenic pressures (population growth, land conversion) and relatively static landscape conditions (proximity to fences, roads and rivers) that create persistent interfaces for human-elephant interaction. The convergence of two methodologically distinct approaches on the same core conclusion, that anthropogenic landscape features and expansion are the primary drivers of HEC, strengthens confidence in this finding. Integrating these complementary perspectives provides a broader understanding of where and under what conditions human-elephant conflict will intensify.

Elephant populations across our study area have been recovering from decades of poaching, but are increasingly limited to a narrower range of available habitat, potentially increasing resource competition and spillovers of elephants into agricultural areas (Stoldt et al., 2020). For example, regions across northwest Botswana where subsistence farming communities share and compete for resources with growing elephant populations are known HEC hotspots and have seen significant increases in HEC over the past two decades (Buchholtz et al., 2023). Our analysis finds that increasing human land use will continue to place pressure on elephants and is likely to drive increased conflict between humans and elephants, emphasizing the risks of elephant range overlap with cropland areas (Guarnieri et al., 2024). Research at the scale of common HEC mitigation techniques like ‘elephant-sensitive’ land use planning, local scout-based monitoring systems, and elephant deterrents can further support local adaptation to HEC (Graham et al., 2010; Jayakody et al., 2024; Karidozo et al., 2016).

This study represents the first analysis explicitly linking future human land use expansion with increases in human-elephant conflict in Southern Africa. Previous research has highlighted the expansion of human land use into elephant ranges (Guarnieri et al., 2024), a

trend that is mirrored in overall human and wildlife populations, which are expected to increase in overlap across 56% of global terrestrial land area through 2070 (Ma et al., 2024). Our finding of a clear causal link between human footprint expansion and rising conflict underscores the concerning predictions of globally-increasing overlap between humans and wildlife species. Research suggests that human-dominated landscapes can provide functional connectivity between less disturbed habitats despite having unsustainably high mortality rates for wildlife (Lamb et al., 2020); however, species persistence does not solve the underlying harms that conflict causes to human lives and livelihoods (Braczkowski et al., 2023; Drake et al., 2021). These livelihood impacts, along with support for long-term conservation measures needed for the preservation of species and natural systems, are of utmost concern for regions experiencing wildlife-induced conflict globally.

Interpretation of our findings should consider key limitations related to data usage, spatial resolution, and assumptions about future environmental and demographic conditions. Our projections assume a static elephant population distribution; future changes in elephant abundance or movement corridors could independently amplify or dampen conflict patterns. Furthermore, the HEC dataset may underreport true occurrences due to gaps in the community-based reporting system, potentially affecting model accuracy. Additionally, land cover data used in this analysis were based on generalized plant functional types, limiting our ability to assess crop-specific variation in raiding risk, which has previously been observed in the eastern Okavango Panhandle of Botswana (Matsika et al., 2023). Lastly, climate projections, while downscaled, may not capture localized orographic and hydrological variation that influences conflict dynamics. A more detailed discussion of these and other limitations, including model fitting considerations and population trend assumptions, is provided in Text S3.

5 Conclusion

The population recovery and ongoing protection of the 300,000 elephants in Southern Africa today (Thouless et al., 2016) represent a positive conservation success story, but conflict with human communities puts this success at risk. Our findings reveal that, without proactive

intervention, HEC in our study area is projected to rapidly increase in number and extent through the end of the century. This has the potential to further impact human lives and livelihoods and undermine the region's recent progress in wildlife conservation. However, our finding that anthropogenic land use outweighs climate factors empowers local decision-makers to shape HEC outcomes through proactive landscape planning, an urgent need as human-wildlife overlap intensifies globally. By identifying drivers and future HEC pathways, we provide crucial information to target mitigation measures, support coexistence, and protect human livelihoods and at-risk species into the coming decades. More broadly, our integrated causal-inference and machine learning framework provides a transferable approach for forecasting and managing human-wildlife conflict under global change.

Ethical Statement

This study used secondary data from the Conservation Information (ConInfo) database, which contains anonymized, aggregated records of human-wildlife conflict events reported at the 2 km grid level. No primary data collection involving human participants or animals was conducted. Data access was granted by the Namibian Association of Community Based Natural Resource Management (NACSO) and the Ministry of Environment, Forestry and Tourism.

Acknowledgments

The authors gratefully acknowledge funding from the John and Jody Arnhold UC Santa Barbara-Conservation International Climate Solutions Collaborative. Additionally, the authors used ChatGPT (GPT-5 series) to assist with language refinement and structural suggestions. All outputs were reviewed and verified by the authors.

Open Research

Replication code and data for this study are provided at (Yu et al., 2025) and can be found at the following doi 10.5281/zenodo.15466230. Analysis was performed in R (version 4.2.1) and we specifically use the `dismo` R package (version 1.3.14) and the `ENMeval` R package (version

2.0.4) for point process model selection and creation, and the 'plm' R package (version 2.6-6) for the fixed effects linear models.

Conflict of Interest Disclosure

Evan Patrick has a consulting relationship with Carbon Direct Inc., a company combining science, technology, and capital to deliver quality carbon dioxide management at scale.

References

Abrahms, B. (2021). Human-wildlife conflict under climate change. *Science*, *373*(6554), 484–485.

Abrahms, B., Carter, N. H., Clark-Wolf, T. J., Gaynor, K. M., Johansson, E., McInturff, A., Nisi, A. C., Rafiq, K., & West, L. (2023). Climate change as a global amplifier of human–wildlife conflict. *Nature Climate Change*, *13*(3), 224–234.

Araujo, D. S., Enquist, B. J., Frazier, A. E., Merow, C., Roehrdanz, P. R., Moulatlet, G. M., Zvoleff, A., Song, L., Maitner, B., & Nikolopoulos, E. I. (2025). Global Future Drought Layers Based on Downscaled CMIP6 Models and Multiple Socioeconomic Pathways. *Scientific Data*, *12*(1), 295.

Braczkowski, A. R., O'Bryan, C. J., Lessmann, C., Rondinini, C., Crysell, A. P., Gilbert, S., Stringer, M., Gibson, L., & Biggs, D. (2023). The unequal burden of human-wildlife conflict. *Communications Biology*, *6*(1), 182.

Branco, P. S., Merkle, J. A., Pringle, R. M., Pansu, J., Potter, A. B., Reynolds, A., Stalmans, M., & Long, R. A. (2019). Determinants of elephant foraging behaviour in a coupled human-natural system: Is brown the new green? *Journal of Animal Ecology*, *88*(5), 780–792.

458 Buchholtz, E. K., McDaniels, M., McCulloch, G., Songhurst, A., & Stronza, A. (2023). A mixed-
459 methods assessment of human-elephant conflict in the Western Okavango Panhandle,
460 Botswana. *People and Nature*, *5*(2), 557–571. https://doi.org/10.1002/pan3.10443
461 Cameron, A. C., Gelbach, J. B., & Miller, D. L. (2011). Robust inference with multiway clustering.
462 *Journal of Business & Economic Statistics*, *29*(2), 238–249.
463 Chen, G., Li, X., & Liu, X. (2022). Global land projection based on plant functional types with a 1-
464 km resolution under socio-climatic scenarios. *Scientific Data*, *9*(1), 125.
465 https://doi.org/10.1038/s41597-022-01208-6
466 Craig, G. C., Gibson, D. S. C., & Uiseb, K. H. (2021). Namibia's elephants—Population,
467 distribution and trends. *Pachyderm*, *62*, 35–52.
468 Dejene, S. W., Mpakairi, K. S., Kanagaraj, R., Wato, Y. A., & Mengistu, S. (2021). Modelling
469 continental range shift of the African elephant (Loxodonta africana) under a changing
470 climate and land cover: Implications for future conservation of the species. *African*
471 *Zoology*, *56*(1), 25–34.
472 Didan, K. (2021). *MODIS/Terra vegetation indices 16-Day L3 global 250m SIN Grid V061. NASA*
473 *EOSDIS land processes distributed active archive center* [Dataset]. Accessed 2023-11-09
474 from https://doi. org/10.5067/MODIS/MOD13Q1. 061.
475 Drake, M. D., Salerno, J., Langendorf, R. E., Cassidy, L., Gaughan, A. E., Stevens, F. R., Pricope, N.
476 G., & Hartter, J. (2021). Costs of elephant crop depredation exceed the benefits of
477 trophy hunting in a community-based conservation area of Namibia. *Conservation*
478 *Science and Practice*, *3*(1), e345.

Fox, J., Weisberg, S., Adler, D., Bates, D., Baud-Bovy, G., Ellison, S., Firth, D., Friendly, M., Gorjanc, G., & Graves, S. (2012). Package 'car.' *Vienna: R Foundation for Statistical Computing*, *16*(332), 333.

Graham, M. D., NOTTER, B., ADAMS, W. M., LEE, P. C., & OCHIENG, T. N. (2010). Patterns of crop-raiding by elephants, Loxodonta africana, in Laikipia, Kenya, and the management of human–elephant conflict. *Systematics and Biodiversity*, *8*(4), 435–445. https://doi.org/10.1080/14772000.2010.533716

Greene, W. H. (2008). The econometric approach to efficiency analysis. *The Measurement of Productive Efficiency and Productivity Growth*, *1*(1), 92–250.

Guarnieri, M., Kumaishi, G., Brock, C., Chatterjee, M., Fabiano, E., Katrak-Adefowora, R., Larsen, A., Lockmann, T. M., & Roehrdanz, P. R. (2024). Effects of climate, land use, and human population change on human–elephant conflict risk in Africa and Asia. *Proceedings of the National Academy of Sciences*, *121*(6), e2312569121.

Haklay, M., & Weber, P. (2008). Openstreetmap: User-generated street maps. *IEEE Pervasive Computing*, *7*(4), 12–18.

Harper, K. L., Lamarche, C., Hartley, A., Peylin, P., Ottlé, C., Bastrikov, V., San Martín, R., Bohnenstengel, S. I., Kirches, G., Boettcher, M., Shevchuk, R., Brockmann, C., & Defourny, P. (2023). *ESA Land Cover Climate Change Initiative (Land_Cover_cci): Global Plant Functional Types (PFT) Dataset, v2.0.8* [Application/xml]. NERC EDS Centre for Environmental Data Analysis. https://doi.org/10.5285/26A0F46C95EE4C29B5C650B129AAB788

Hersbach, H., Bell, B., Berrisford, P., Hirahara, S., Horányi, A., Muñoz-Sabater, J., Nicolas, J., Peubey, C., Radu, R., & Schepers, D. (2020). The ERA5 global reanalysis. *Quarterly Journal of the Royal Meteorological Society*, *146*(730), 1999–2049.

Homdee, T., Pongput, K., & Kanae, S. (2016). A comparative performance analysis of three standardized climatic drought indices in the Chi River basin, Thailand. *Agriculture and Natural Resources*, *50*(3), 211–219.

Huang, R. M., Maré, C., Guldemond, R. A., Pimm, S. L., & van Aarde, R. J. (2024). Protecting and connecting landscapes stabilizes populations of the Endangered savannah elephant. *Science Advances*, *10*(1), eadk2896. https://doi.org/10.1126/sciadv.adk2896

Huang, R. M., van Aarde, R. J., Pimm, S. L., Chase, M. J., & Leggett, K. (2022). Mapping potential connections between Southern Africa's elephant populations. *Plos One*, *17*(10), e0275791.

Jayakody, S., Estacio, I., Sianipar, C. P. M., Onitsuka, K., Basu, M., & Hoshino, S. (2024). Maxent modeling for predicting the potential distribution of human-elephant conflict risk in Sri Lanka. *Applied Geography*, *173*, 103447. https://doi.org/10.1016/j.apgeog.2024.103447

Jones, B. (2010). The evolution of Namibia's communal conservancies. In *Community rights, conservation and contested land* (pp. 106–120). Routledge.

Karger, D. N., Conrad, O., Böhner, J., Kawohl, T., Kreft, H., Soria-Auza, R. W., Zimmermann, N. E., Linder, H. P., & Kessler, M. (2017). Climatologies at high resolution for the earth's land surface areas. *Scientific Data*, *4*(1), 170122. https://doi.org/10.1038/sdata.2017.122

Karidozo, M., La Grange, M., & Osborn, F. V. (2016). Assessment of the human wildlife conflict mitigation measures being implemented by the Kavango-Zambezi Transfrontier

Conservation Area (KAZA TFCA) partner countries. *Report to the KAZA TFCA Secretariat (BMZ No.: 2009 66 788 and BMZ No.: 2006 65 646), Kasane, Botswana*.

Lamb, C. T., Ford, A. T., McLellan, B. N., Proctor, M. F., Mowat, G., Ciarniello, L., Nielsen, S. E., & Boutin, S. (2020). The ecology of human–carnivore coexistence. *Proceedings of the National Academy of Sciences*, *117*(30), 17876–17883.

Lehner, B., & Grill, G. (2013). Global river hydrography and network routing: Baseline data and new approaches to study the world's large river systems: GLOBAL RIVER HYDROGRAPHY AND NETWORK ROUTING. *Hydrological Processes*, *27*(15), 2171–2186. https://doi.org/10.1002/hyp.9740

Li, M., Zhou, B.-B., Gao, M., Chen, Y., Hao, M., Hu, G., & Li, X. (2022). Spatiotemporal dynamics of global population and heat exposure (2020–2100): Based on improved SSP-consistent population projections. *Environmental Research Letters*, *17*(9), 094007. https://doi.org/10.1088/1748-9326/ac8755

Loarie, S. R., van Aarde, R. J., & Pimm, S. L. (2009). Elephant seasonal vegetation preferences across dry and wet savannas. *Biological Conservation*, *142*(12), 3099–3107.

Ma, D., Abrahms, B., Allgeier, J., Newbold, T., Weeks, B. C., & Carter, N. H. (2024). Global expansion of human-wildlife overlap in the 21st century. *Science Advances*, *10*(34), eadp7706.

Matsika, T. A., Masunga, G. S., Makati, A., McCulloch, G., Stronza, A., Songhurst, A. C., Adjetey, J. A., & Obopile, M. (2023). Crop diversity and susceptibility of crop fields to elephant raids in eastern Okavango Panhandle, northern Botswana. *Ecology and Evolution*, *13*(3), e9910. https://doi.org/10.1002/ece3.9910

MEFT, & NACSO. (2022). *The state of community conservation in Namibia (Annual Report 2022)*.

Merow, C., Smith, M. J., Edwards, T. C., Guisan, A., McMahon, S. M., Normand, S., Thuiller, W., Wüest, R. O., Zimmermann, N. E., & Elith, J. (2014). What do we gain from simplicity versus complexity in species distribution models? *Ecography*, *37*(12), 1267–1281. https://doi.org/10.1111/ecog.00845

Merow, C., Smith, M. J., & Silander, J. A. (2013). A practical guide to MaxEnt for modeling species' distributions: What it does, and why inputs and settings matter. *Ecography*, *36*(10), 1058–1069. https://doi.org/10.1111/j.1600-0587.2013.07872.x

Mukeka, J. M., Ogutu, J. O., Kanga, E., & Røskaft, E. (2019). Human-wildlife conflicts and their correlates in Narok County, Kenya. *Global Ecology and Conservation*, *18*, e00620. https://doi.org/10.1016/j.gecco.2019.e00620

Munyao, M., Siljander, M., Johansson, T., Makokha, G., & Pellikka, P. (2020). Assessment of human–elephant conflicts in multifunctional landscapes of Taita Taveta County, Kenya. *Global Ecology and Conservation*, *24*, e01382. https://doi.org/10.1016/j.gecco.2020.e01382

Mwangi, D. K., Akinyi, M., Maloba, F., Ngotho, M., Kivai, S., Kagira, J., & Ndeereh, D. (2016). Socioeconomic and health implications of human wildlife interactions in Nthongoni, Eastern Kenya. *African Journal of Wildlife Research*, *46*(2), 87–102.

Naha, D., Sathyakumar, S., Dash, S., Chettri, A., & Rawat, G. S. (2019). Assessment and prediction of spatial patterns of human-elephant conflicts in changing land cover scenarios of a human-dominated landscape in North Bengal. *PLOS ONE*, *14*(2), e0210580. https://doi.org/10.1371/journal.pone.0210580

566 Nettleton, D. (2014). Chapter 6—Selection of Variables and Factor Derivation. In D. Nettleton
567 (Ed.), *Commercial Data Mining* (pp. 79–104). Morgan Kaufmann.
568 https://doi.org/10.1016/B978-0-12-416602-8.00006-6
569 Nsonsi, F., Heymans, J.-C., Diamouangana, J., Mavinga, F. B., & Breuer, T. (2018). Perceived
570 human–elephant conflict and its impact for elephant conservation in northern Congo.
571 *African Journal of Ecology*, *56*(2), 208–215.
572 O'Connell-Rodwell, C. E., Rodwell, T., Rice, M., & Hart, L. A. (2000). Living with the modern
573 conservation paradigm: Can agricultural communities co-exist with elephants? A five-
574 year case study in East Caprivi, Namibia. *Biological Conservation*, *93*(3), 381–391.
575 Oehlert, G. W. (1992). A note on the delta method. *The American Statistician*, *46*(1), 27–29.
576 Pearson, R. (2010). *Species' Distribution Modeling for Conservation Educators and Practitioners*.
577 https://www.semanticscholar.org/paper/Species%E2%80%99-Distribution-Modeling-
578 for-Conservation-and-Pearson/c8ccf4e7187ee37454ac2a350d9a8e22bef6ba85
579 Phillips, S. J., Anderson, R. P., Dudík, M., Schapire, R. E., & Blair, M. E. (2017). Opening the black
580 box: An open-source release of Maxent. *Ecography*, *40*(7), 887–893.
581 https://doi.org/10.1111/ecog.03049
582 Phillips, S. J., Anderson, R. P., & Schapire, R. E. (2006). Maximum entropy modeling of species
583 geographic distributions. *Ecological Modelling*, *190*(3), 231–259.
584 https://doi.org/10.1016/j.ecolmodel.2005.03.026
585 Rani, M., Panda, D., Allen, M. L., Pandey, P., Singh, R., & Kumar Singh, S. (2024). Assessment and
586 prediction of human-elephant conflict hotspots in the human-dominated area of Rajaji-

Corbett landscape, Uttarakhand, India. *Journal for Nature Conservation*, *79*, 126601. https://doi.org/10.1016/j.jnc.2024.126601

Shaffer, L. J., Khadka, K. K., Van Den Hoek, J., & Naithani, K. J. (2019). Human-Elephant Conflict: A Review of Current Management Strategies and Future Directions. *Frontiers in Ecology and Evolution*, *6*. https://doi.org/10.3389/fevo.2018.00235

Smith, R. J., & Kasiki, S. M. (2000). A spatial analysis of human–elephant conflict in the Tsavo ecosystem, Kenya. *AfESG Report. IUCN/SSC, Gland, Switzerland*.

Stoldt, M., Göttert, T., Mann, C., & Zeller, U. (2020). Transfrontier Conservation Areas and Human-Wildlife Conflict: The Case of the Namibian Component of the Kavango-Zambezi (KAZA) TFCA. *Scientific Reports*, *10*(1), Article 1. https://doi.org/10.1038/s41598-020-64537-9

Thant, Z. M., May, R., & Røskaft, E. (2021). Pattern and distribution of human-elephant conflicts in three conflict-prone landscapes in Myanmar. *Global Ecology and Conservation*, *25*, e01411.

Thouless, C., Dublin, H. T., Blanc, J., Skinner, D. P., Daniel, T. E., Taylor, R., Maisels, F., Frederick, H., & Bouché, P. (2016). African elephant status report 2016. *Occasional Paper Series of the IUCN Species Survival Commission*, *60*, 309.

Tsalyuk, M., Kilian, W., Reineking, B., & Getz, W. M. (2019). Temporal variation in resource selection of African elephants follows long-term variability in resource availability. *Ecological Monographs*, *89*(2), e01348.

UNEP-WCMC, I. (2024). *Protected planet: The world database on protected areas*.

US Geological Survey. (2010). *Global Multi-resolution Terrain Elevation* [Dataset].

609 Wenborn, M. J., Katjimbari, R., Tjiseua, J., Muheue, K., Tjimuine, U., Muundjua, S. T., Svensson,
610 M. S., & Nijman, V. (2025). Assessment of Mitigation of Human–Elephant Conflict in the
611 Highlands of Northwest Namibia. *The Journal of Environment & Development*,
612 10704965241311353.
613 WorldPop, & Bondarenko, M. (2020). *Individual Countries 1km Population Density (2000-2020)*
614 [Dataset]. University of Southampton. https://doi.org/10.5258/SOTON/WP00674
615 Yu, C., Patrick, E., & Pepperdine, M. (2025). *Data and Replication Code for An expanding human*
616 *footprint will escalate human-elephant conflict in a Southern African landscape through*
617 *the end of the century* [Dataset]. Zenodo. https://doi.org/10.5281/zenodo.15466231.
618

Figures and Tables

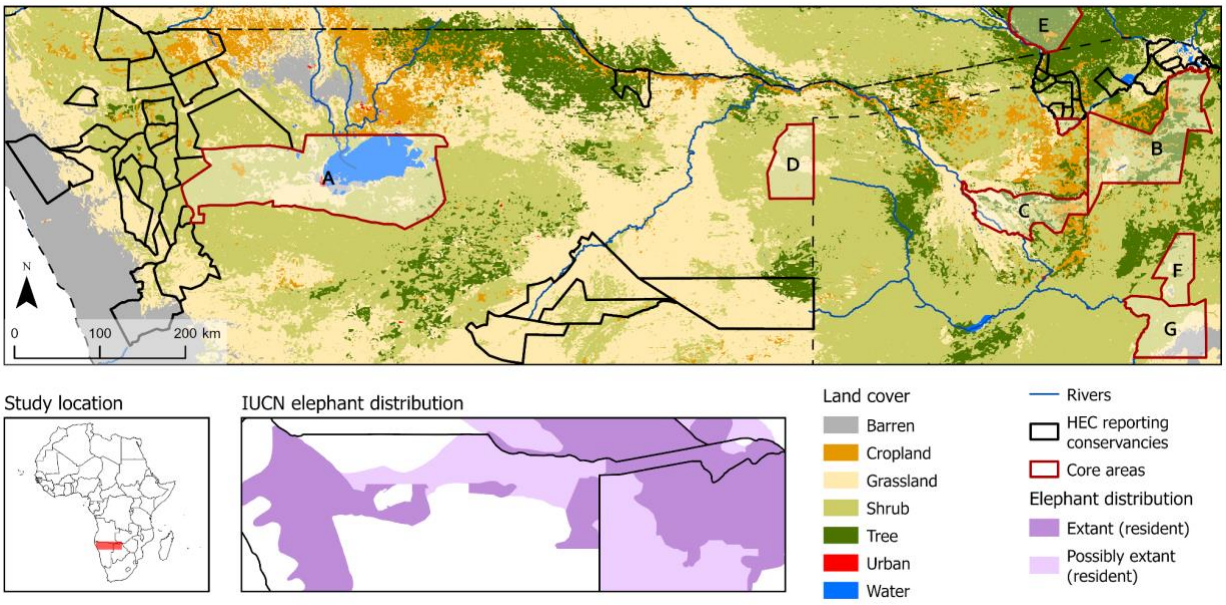

Figure 1. Study area extent. Land cover data are from Chen et al. (2022), showing land cover types in 2015. Rivers are from the HydroRivers dataset defined as greater than ord_flow 5 (10 km^2 or an average river flow of at least 0.1 m^3/s). Core area boundaries were sourced from the WDPA dataset (UNEP-WCMC, 2024) and identified from (1). They are: A) Etosha National Park; B) Chobe; C) Moremi; D) Khaudum; E) Sioma Ngwezi; F) Nxai Pan; G) Makgadikgadi Pans. The core area adjacent to the top left corner of Chobe (B) is Nkasa Rupara.

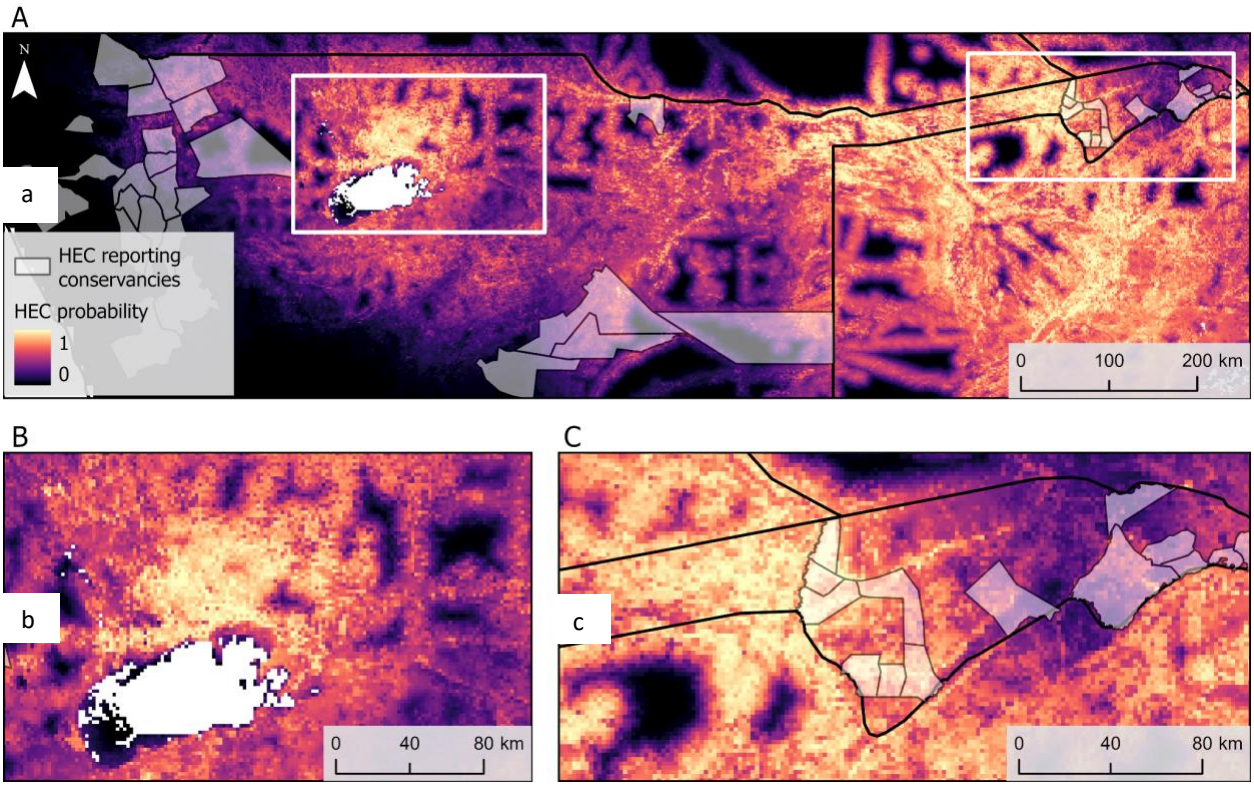

627

628 **Figure 2.** Baseline predictions for the probability of elephant crop raiding during the 2020 wet
629 season. The entire extent of the point process model predictions (a) is the same extent as
630 Figure 1, generated by creating a bounding box (Figure S1) around all HEC reporting communal
631 conservancies (white polygons). HEC reporting conservancies are all Namibian communal
632 conservancies that reported incidents of HEC in the conflict data set used in the analysis. Two
633 predicted HEC risk hotspots are shown in the inset maps: regions north of Etosha National Park
634 (b) in northwest Namibia and the Zambezi Region (c) in northeast Namibia. The white spot in
635 panel b is Etosha Pan, a large salt pan covering almost a quarter of Etosha National Park.

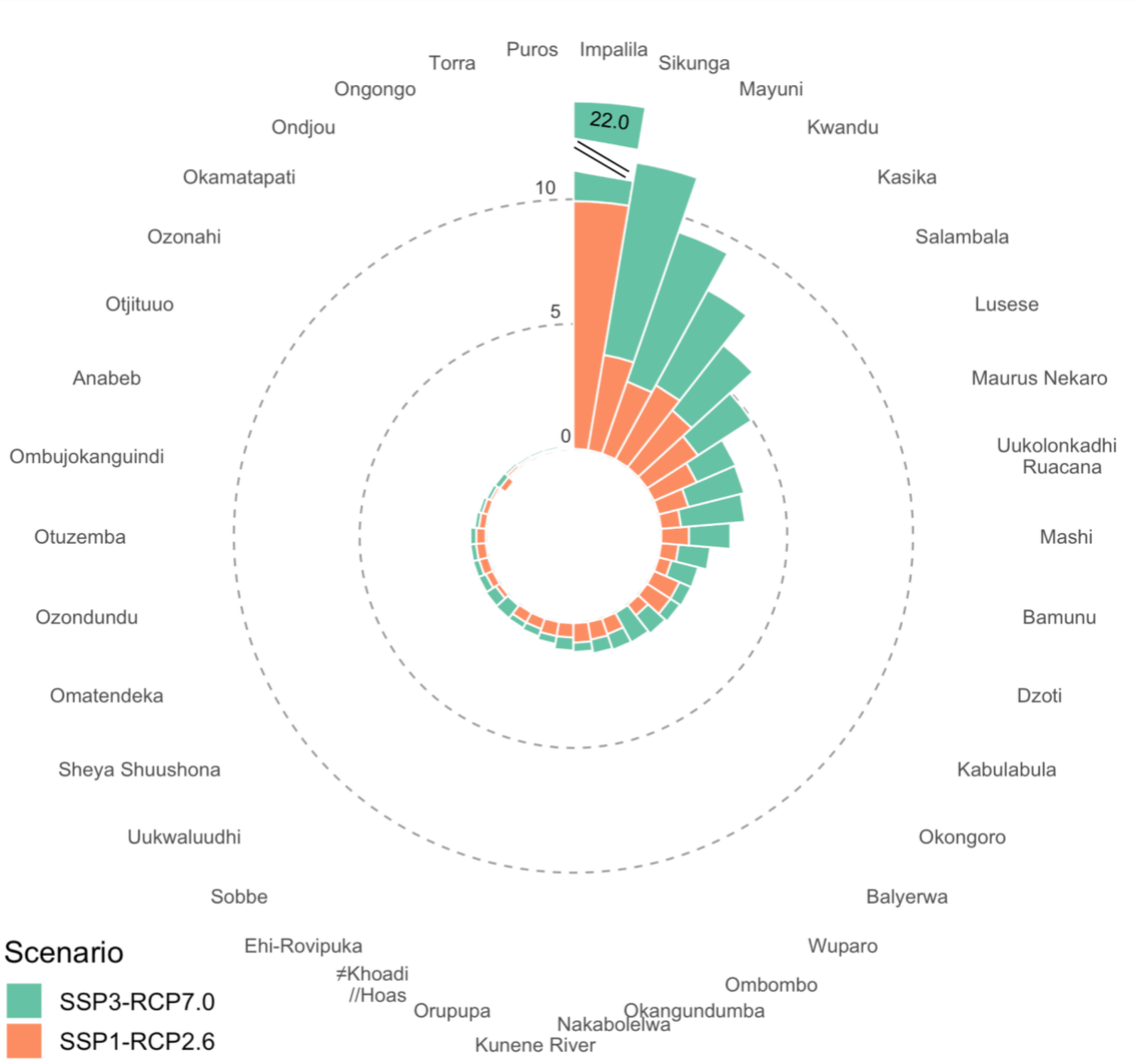

Figure 3. Projections of average grid-level change in HEC events by reporting conservancy, with SSP1-RCP2.6 ("sustainability") and SSP3-RCP7.0 ("regional rivalry") projections stacked. Change values for each conservancy are provided in Table S7. See Figure S9 to see the spatial distribution of change values by each reporting conservancy. Figure S16 shows the location of all conservancies that reported HEC across Namibia.

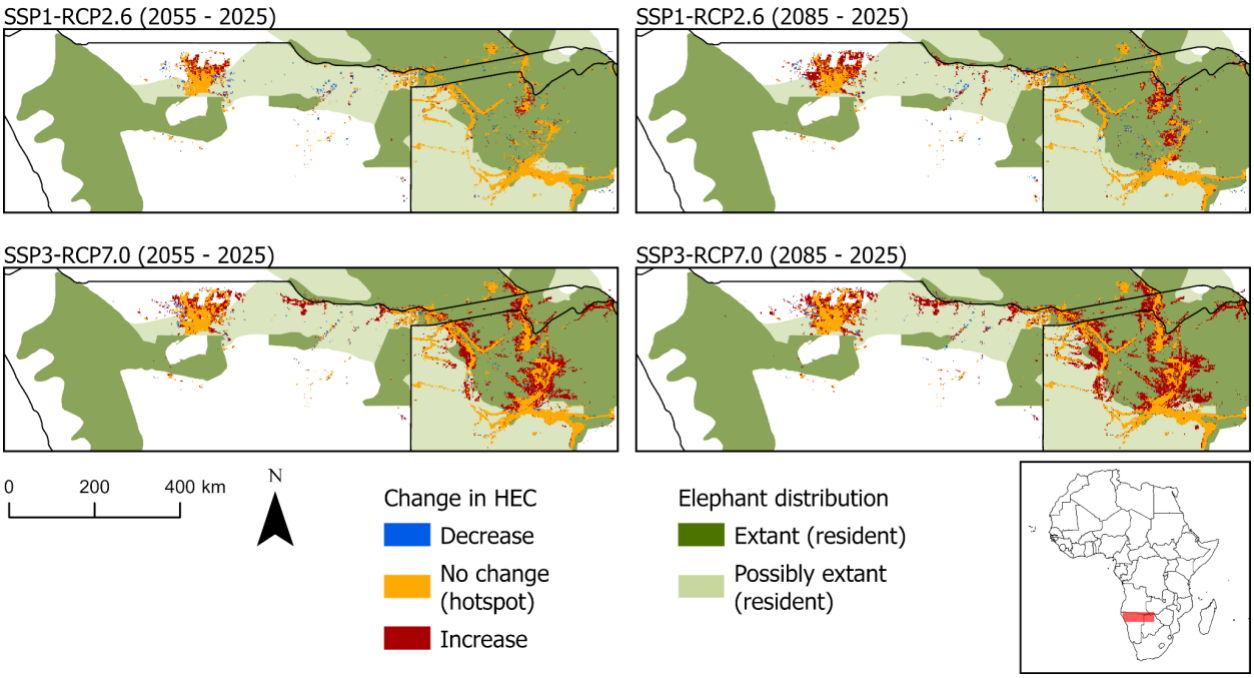

642

643 **Figure 4.** Change in the distribution of crop raiding HEC during the wet season from 2025 to
644 2055 and from 2025 to 2085 under two future scenarios: SSP1-RCP2.6 ("sustainability") and
645 SSP3-RCP7.0 ("regional rivalry"). Continuous HEC predictions were converted to binary
646 outcomes (presence or absence of HEC) using the threshold (0.72) that maximized Cohen's
647 Kappa statistic for the point process model. African elephant distribution from the IUCN is
648 overlaid to compare model results with extant (dark green) and possibly extant (light green)
649 delineations. All regions not colored in the figure were consistent "coldspots" of HEC (i.e., areas
650 with an HEC probability less than 0.72 in both periods being compared).

Scaled Covariate	Crop Raiding Model Outputs	
	Wet Season	Dry Season
Grid spei3	-0.012 (0.016)	0.001 (0.001)
50km spei3	0.014 (0.021)	-0.003 (0.002)
Core spei3	**-0.081*** **(0.037)**	0.003 (0.003)
Population	**0.176***** **(0.028)**	**0.011***** **(0.002)**
Tree Cover	-0.019 (0.017)	-0.004 (0.003)
Cropland Cover	**0.053***** **(0.012)**	0.001 (0.001)
Built Cover	**0.022**** **(0.006)**	0.001 (0.001)
Fixed Effects		
Spatial Group	Yes	Yes
Season-Year	Yes	Yes
Observations	126,304	126,304

Table 1. Fixed effects regression estimates for crop raiding models with standard errors, clustered on spatial group and season-year, in parentheses below. Covariates were scaled to a consistent 0-1 range before running the regression, allowing for comparable coefficients within models. Grid spei3 is the 3-month SPEI calculated at the HEC grid level, 50km spei3 represents 3-month SPEI values at a 50 km buffer around the HEC grid, and core spei3 is 3-month SPEI values in the nearest elephant core area. Population represents yearly human population counts sourced from WorldPop. Tree, cropland, and built cover are the percentage cover for each land cover type, sourced from the Copernicus Climate Change Initiative (CCI) Global Plant Functional Type dataset. * signifies a p-value of <0.05, ** refers to <0.01, and *** denotes <0.001.

Supplementary Information for

An expanding human footprint will escalate human-elephant conflict in a Southern African landscape through the end of the century

E. Patrick[1], M. Pepperdine[1], C. Yu[1], S. Pesek[2], O. Somhegyi[3], J. Krieger[4], N. McManus[4], E. Fabiano[5], C. Sikopo[6], P. Roehrdanz[4], A. Larsen[1]

[1]Bren School of Environmental Science & Management, University of California, Santa Barbara, 93106-5131, USA. [2]Energy and Resources Group, University of California, Berkeley, 345 Giannini Hall, Berkeley, CA 94720, USA. [3]Conservation Biology Institute, 136 SW Washington Ave., Corvallis, OR 97333, USA. [4]The Moore Center for Science and Solutions, Conservation International, 2011 Crystal Dr., Arlington, VA, 22202, USA. [5]Department of Wildlife Management and Tourism Studies, University of Namibia, Katima Mulilo 1096, Namibia. [6]Ministry of Environment, Forestry and Tourism, Windhoek 13306, Namibia

Corresponding Author: Evan Patrick (epatrick@ucsb.edu)

Other supplementary materials for this manuscript include the following:

Text S1 to S3
Figures S1 to S16
Tables S1 to 10

Introduction

In this supporting information document, we provide information detailing the regression and maximum entropy analyses performed in this manuscript. This includes further analyses performed, such as random effects and count regression specifications, and information on the point process / maximum entropy variable and model selection. We provide a more detailed description of the limitations of the analysis to supplement the brief limitations discussion provided in the main manuscript text. Additionally, further data is provided on the study system and conservancies analyzed in this study.

Text S1.

Alternative Regression Specifications

Crop-raiding events are recorded as non-negative integers that are highly skewed toward zero (Table S1). Treating these data with ordinary least-squares assumes a continuous, homoscedastic, and normally distributed error term. These assumptions may not hold in the context of the HEC event data presented in this analysis. Count regression models were

therefore estimated in parallel to the linear fixed-effects analyses to ensure that our inference is robust to the true distributional nature of the response.

Poisson fixed-effects models provide a natural starting point because they are derived from the Poisson process that underlies many arrival-rate phenomena, including rare wildlife-human interactions. However, the variance of crop-raiding counts exceeds the mean (over-dispersion), an issue that inflates Type I error rates in a pure Poisson framework. We therefore also report negative binomial fixed-effects estimates, which introduce an extra dispersion parameter to accommodate unobserved heterogeneity among grid cells and seasons.

Using fixed effects in both Poisson and negative binomial settings retains the key advantage of our linear specification, control for all time-invariant spatial attributes and year-specific shocks, while allowing the conditional mean function to follow the log-link that is appropriate for counts. Comparing coefficient signs, significance, and marginal effects across linear, Poisson, and negative binomial models highlights where conclusions are robust versus sensitive to distributional assumptions. Table S2 and Table S3 present these count-based results, showing a consistent sensitivity to population across seasons, and cropland cover for wet season regressions, aligning with our linear regression results. Built cover was not significant to $p<0.05$ under either specification but did demonstrate a $p<0.10$ for the Poisson - wet season model.

Alongside the two-way fixed effects (FE) regressions presented in the main text, we also estimated random effects (RE) panel regressions for both wet and dry season crop-raiding models. While FE models have the advantage of controlling for all time-invariant unobserved heterogeneity within spatial groups, they also difference out the effects of time-invariant predictors (e.g., topography, long-term infrastructure placement) that may be ecologically important for understanding human-elephant conflict (HEC). RE models retain these predictors by allowing the unit-specific intercepts (random effects) to vary across spatial groups while assuming independence between the unobserved effects and the included covariates. This enables the inclusion of both within-group temporal variation and between-group cross-sectional variation, potentially offering a fuller picture of the correlates of HEC risk.

We assessed the appropriateness of RE specifications using the Hausman test, which evaluates whether the RE assumption of independence between unobserved effects and regressors holds. For wet-season crop raiding, the Hausman test rejected RE in favor of FE ($p < 0.05$), indicating that unobserved heterogeneity is likely correlated with key predictors in that season; these results should therefore be interpreted with caution. For dry-season crop raiding, the test did not reject RE, suggesting that the RE estimator is consistent in this case. Including the RE models alongside FE allows us to explore the role of time-invariant spatial characteristics, such as elevation, slope, and distances to roads, rivers, and fences, while directly comparing how results differ when causal identification relies solely on within-unit temporal changes (FE) versus when both within- and between-unit variation inform the estimates (RE). Results for both wet and dry season RE models are presented in Table S4.

Text S2.

Point Proess Model Selection and Evaluation

We used the `ENMeval` R package (version 2.0.4) to generate and evaluate a series of point process (alternatively, Maximum Entropy or MaxEnt) models before selecting the 'best' performing model. Two feature class combinations, linear (L) and linear + quadratic (LQ), were used, with regularization multiplier values ranging from 0.5 to 3 in increments of 0.5, to generate a total of 12 models. Using omission rate (OR) and AUC scores as evaluation metrics, the point process model with LQ features and a regularization multiplier of 1 performed the best in the crop raiding model for both the wet (Figure S4) and dry seasons. A single point process model with these parameters was then generated using the `dismo` R package (version 1.3.14), which we used to produce baseline and future predictions of crop raiding HEC events across the study area.

As mentioned, omission rate (OR) and the area under the receiver operating characteristic curve (AUC) were used to assess the models' predictive performance. OR quantifies the proportion of observed presences that are incorrectly predicted as absences, with lower values indicating better model performance (Phillips et al. 2006; Pearson, 2010). AUC assesses how accurately a model determines presences compared to random prediction (i.e., the model's ability to distinguish presence locations from background points). Values range from 0 to 1, where values less than 0.5 imply the prediction is worse than random, 0.5 implies random prediction, and 1 implies perfect prediction (Phillips et al. 2006; Pearson, 2010).

Text S3.

Study Limitations

This study has various limitations related to data usage and modeling efforts. The reporting system used to generate the HEC dataset likely does not capture all HEC occurrences within registered communal conservancies. This may affect fixed-effects and point process model fitting and prediction accuracy, especially if areas with occurrences are measured as having none. However, given the large number of occurrences generated across our study area and period, the omission of some true HEC events is unlikely to significantly impact our results. As with any modeling approach, limitations arise from the parameter selection used to fit and train models. In point process modeling, a key challenge is balancing model complexity to prevent overfitting or underfitting. To mitigate overfitting, we restricted model features to L and LQ. Additionally, we selected the best-performing model based on OR and AUC evaluation metrics. Slight variations in feature class selection or alternative model evaluation criteria (e.g., AIC and BIC) could yield different baseline and future projections when extrapolating point process models to novel combinations of future projections of environmental variables (Merow et al. 2013).

Another limitation concerns land cover data. We relied on a general land cover map with broadly defined plant functional types, using a % cropland indicator to analyze the effects of all crop types on HEC occurrence. This approach does not account for spatial variation in crop-

raiding risk across different crop types, which has been observed in the eastern Okavango Panhandle of Botswana (Matsika et al, 2023). More detailed land use datasets that distinguish between crop types could provide finer-scale insights into HEC spatial patterns.

We find that spatial differences in wetness between core areas and grid-level SPEI are predictive of conflict. However, many climate models do not have the spatial specificity to pick up these changes, with downscaling to local conditions often being an imperfect attempt to reflect realized orographic conditions. While the data we use represent some of the best available in downscaled climate information, we are not confident that we have achieved the spatial specificity needed to understand landscape-level differences in weather that could drive conflict. Finally, our analysis relies on the assumption that elephant populations will remain relatively stable over the coming decades. Analyses such as (Huang et al., 2024) have shown that elephant populations across northern Namibia have been growing in recent decades, a trend that could further accelerate opportunities for HEC.

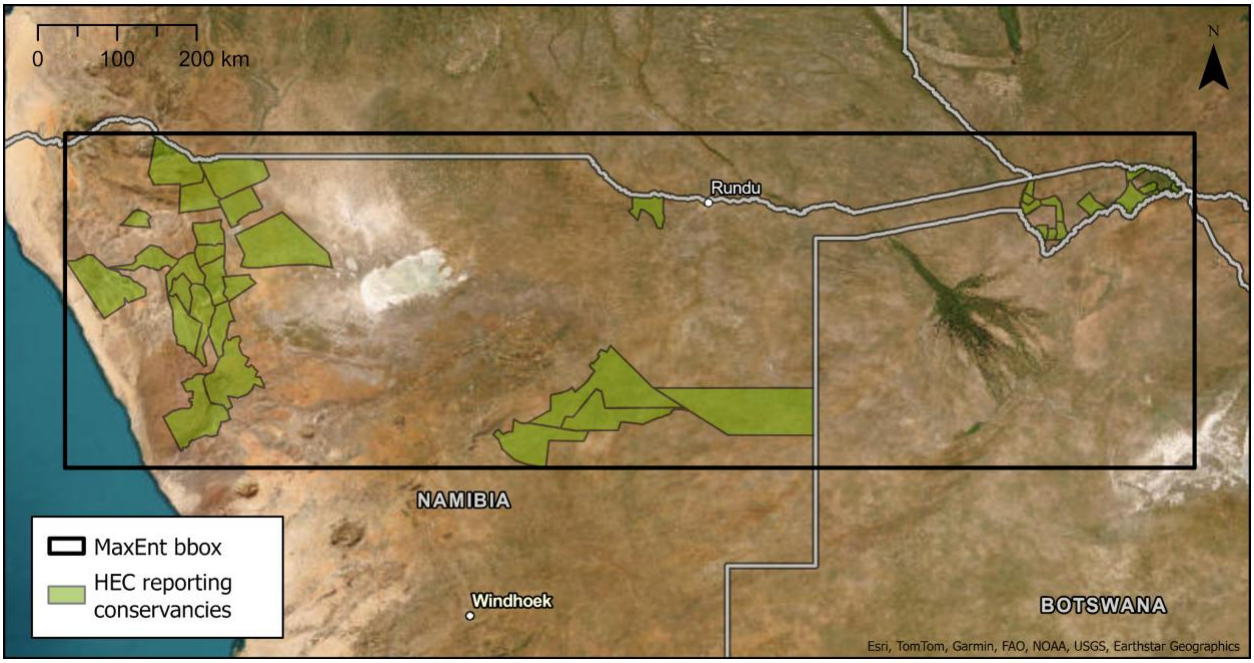

Fig. S1. Bounding box (black outline) used to define the extent to which baseline and future point process model predictions of crop raiding HEC probability were projected. Models were trained using HEC occurrence data from within HEC-reporting Namibian communal conservancies (green) and projected across the broader landscape defined by the bounding box (20.900°S to 17.133°S; 12.499°E to 25.283°E). This area encompasses northern Namibia and Botswana, as well as small portions of Angola and Zambia.

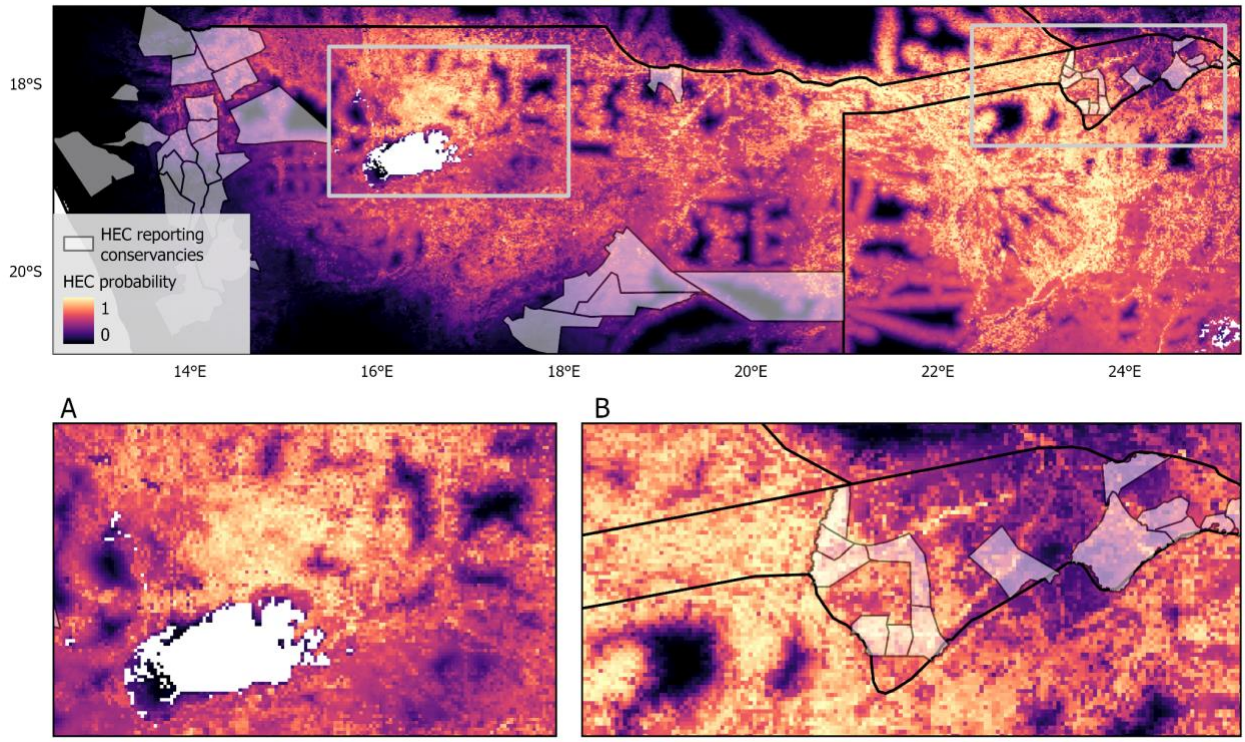

Fig. S2. Baseline predictions for crop raiding HEC probability during the 2020 dry season. Two predicted HEC risk hotspots are shown in the inset maps: regions north of the eastern side of Etosha National Park (A) in northwest Namibia and the Zambezi Region (B) in northeast Namibia.

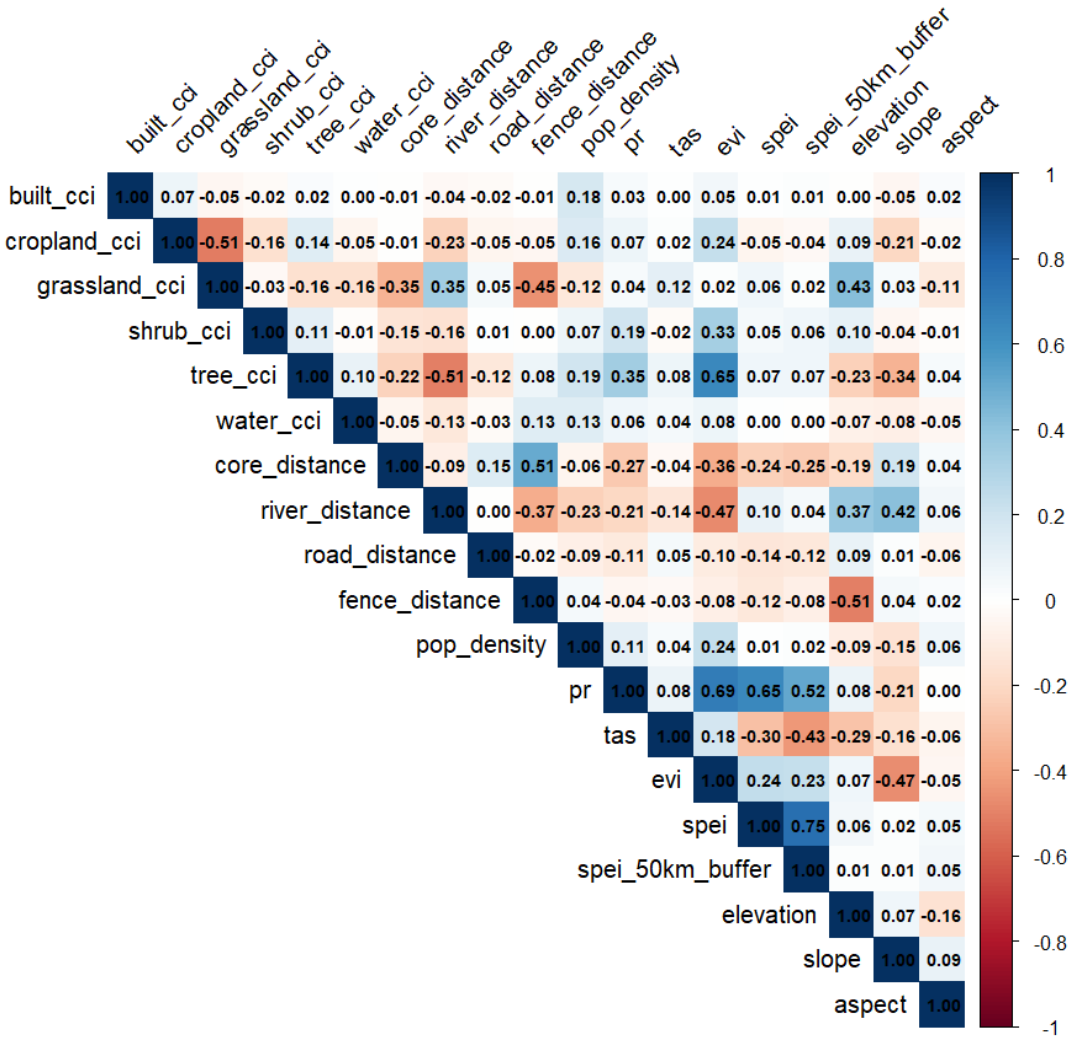

Fig. S3. Pearson's correlation matrix for all environmental predictor variables considered in the point process models.

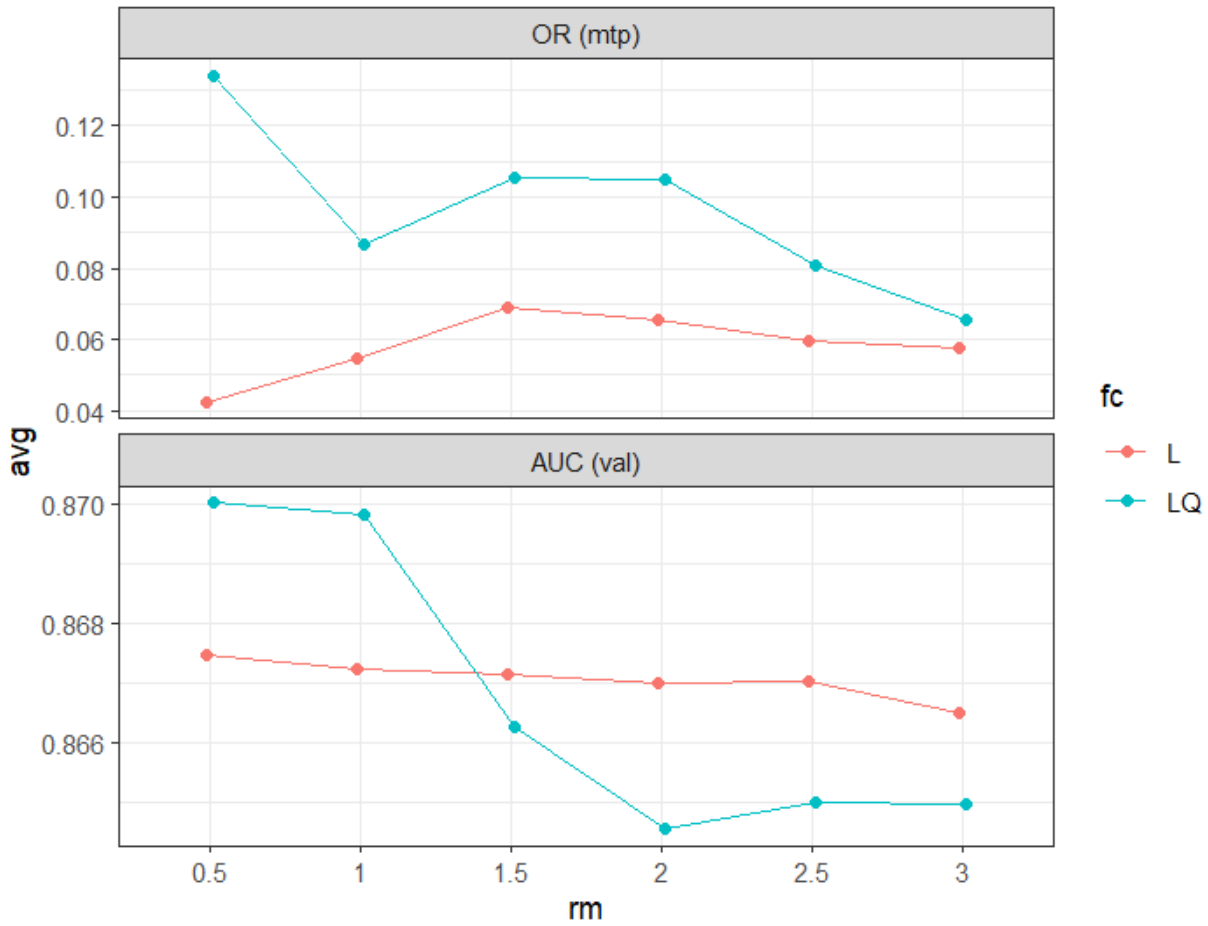

Fig. S4. Evaluation metrics used to select the best-performing point process model with crop raiding occurrences during the wet season.

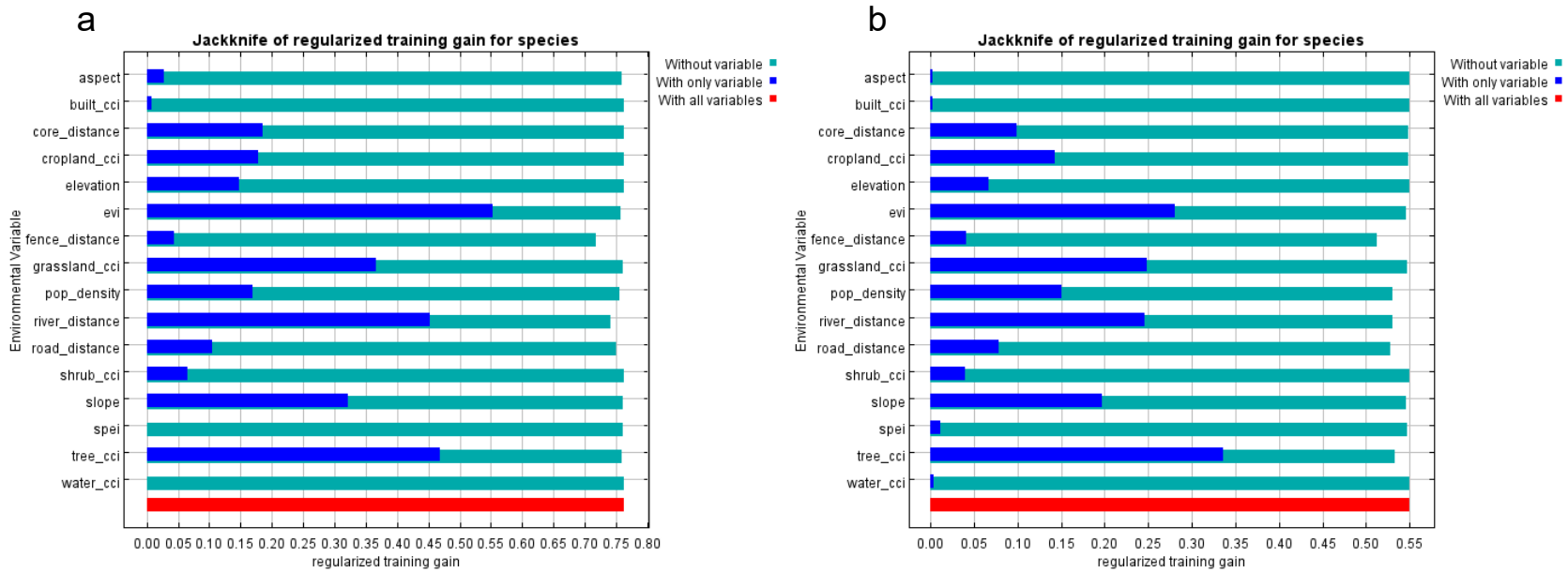

Fig. S5. Jackknife of regularized training gain for all environmental variables used in the **(a)** crop raiding, wet season point process model and **(b)** crop raiding, dry season point process model. Dark blue shows the regularized training gain with only that variable, teal without that variable, and red with all variables. If a variable alone has high training gain (blue), it's highly predictive by itself. If the training gain drops significantly when a variable is removed (teal), that variable contributes a lot to the collective model.

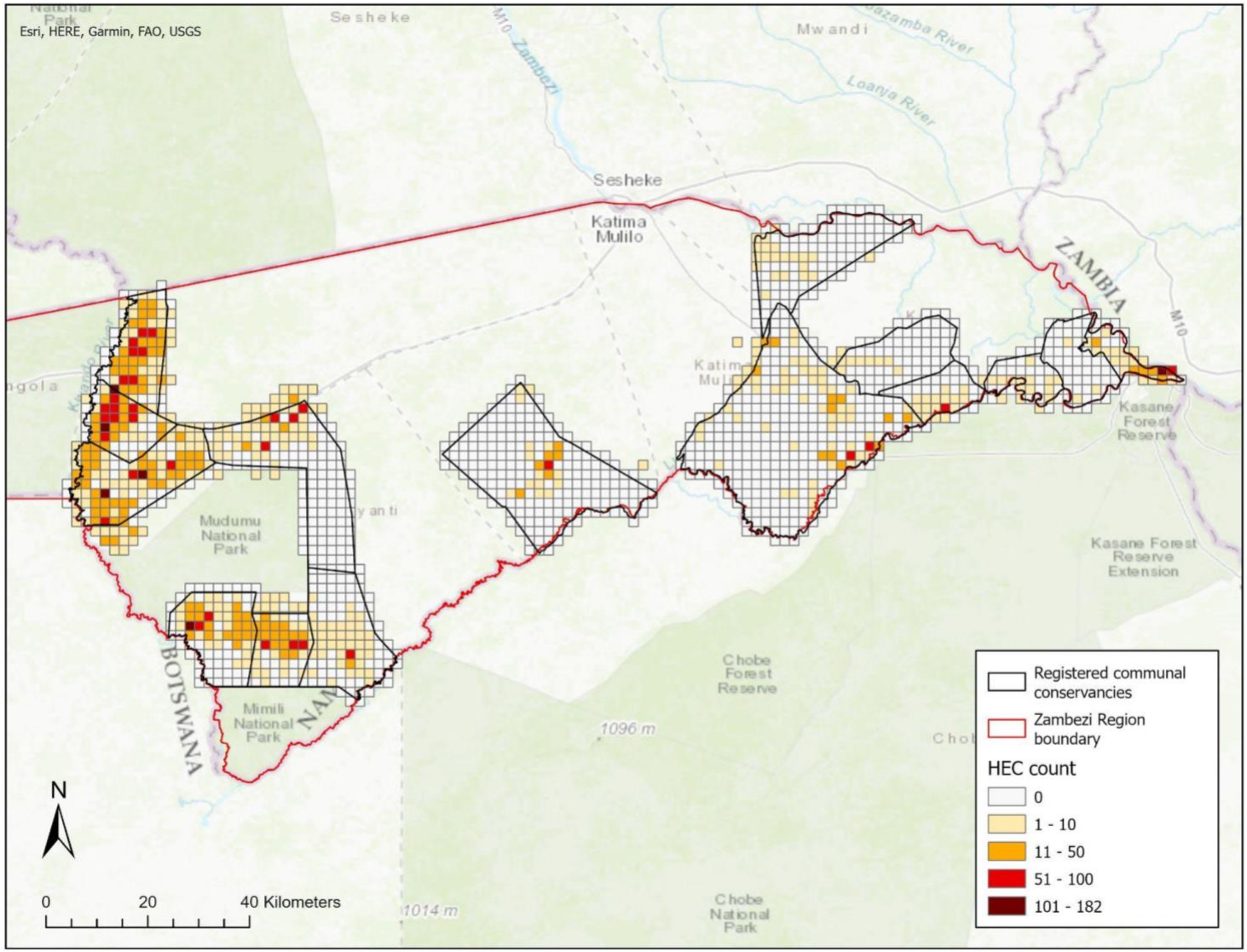

Fig. S6. HEC data used in the regression and point process model analyses. Conflict counts are shown for 2004-2020, with higher conflict counts represented by darker shades of red.

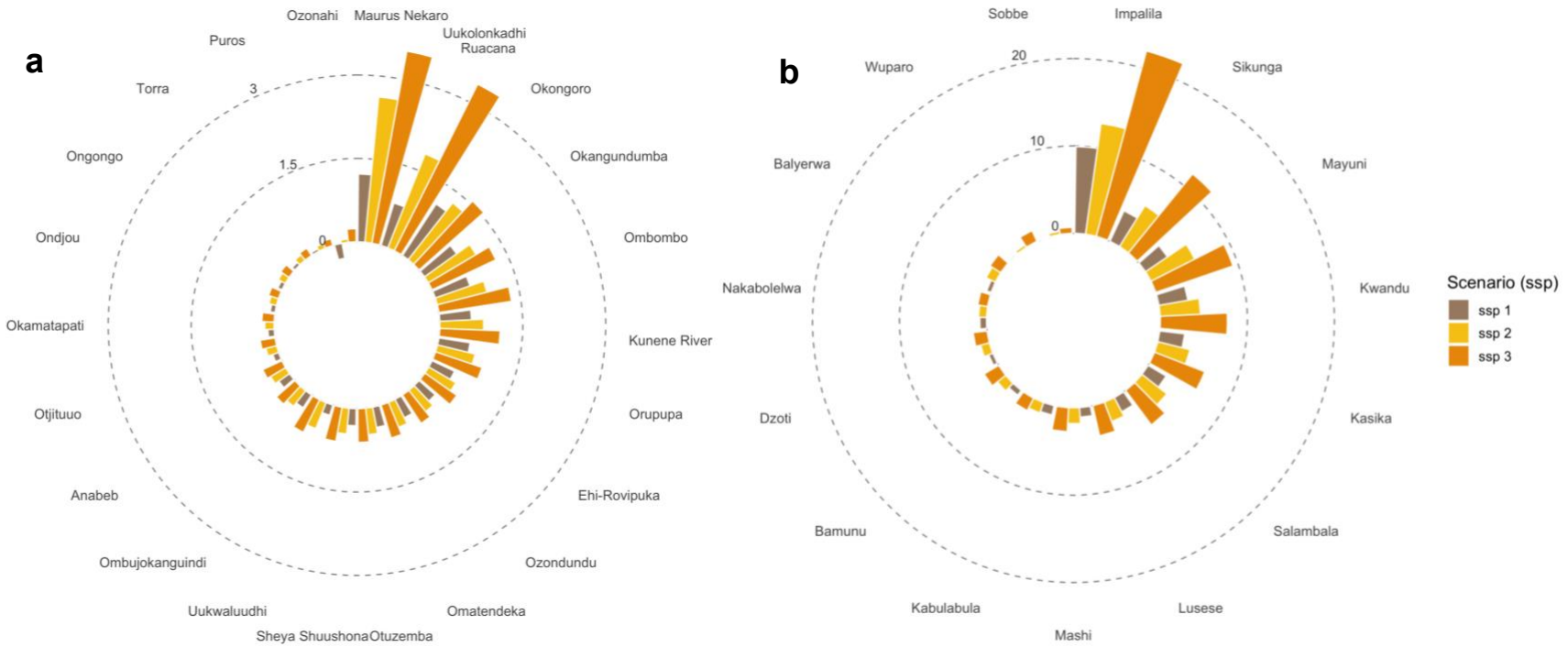

Fig. S7. Rose plots of average change in Wet Season Crop Raiding events (per grid cell) from 2025-2085 by conservancy and split by region. Panel **a** on the left shows results from Western Namibia, split by conservancy, across SSPs 1, 2, and 3. Panel **b** shows the same results for conservancies in the Zambezi region, which showed much more dramatic increases in conflict.

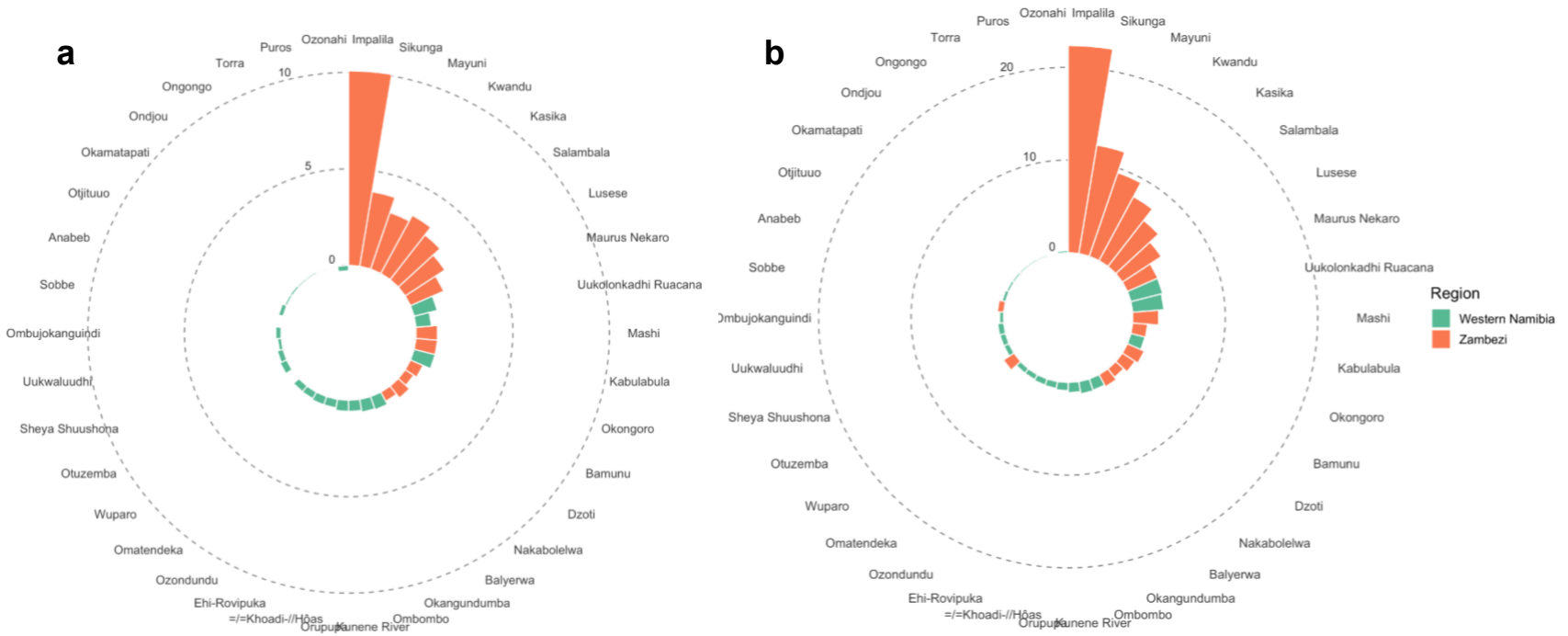

Fig. S8. Rose plots of average grid-cell change in wet season crop raiding events per conservancy from 2025-2085, colored by region. Panel **a** shows results from SSP 1, whereas panel **b** shows results from SSP 3. Note that the scale of b is double that of a.

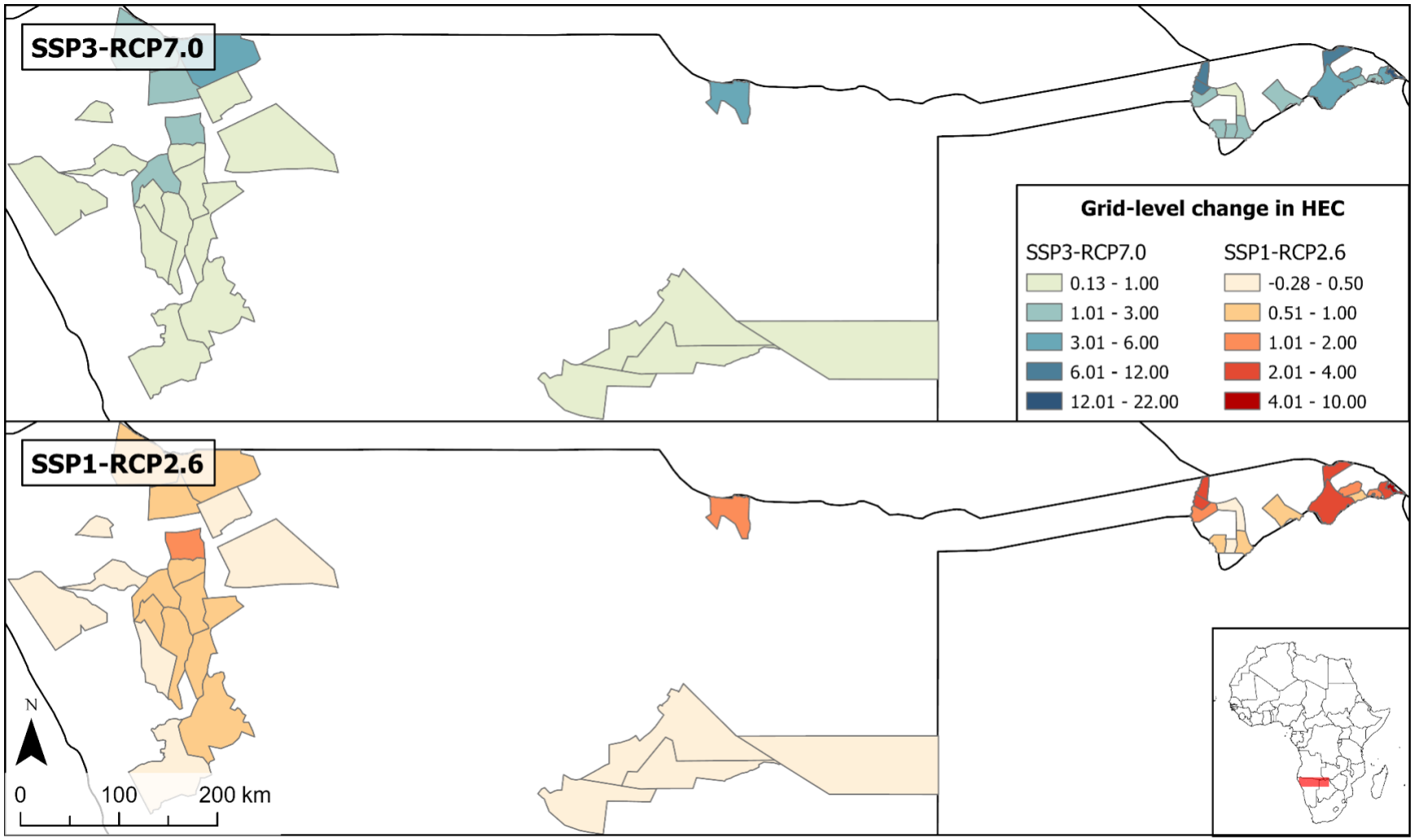

Fig. S9. HEC reporting communal conservancies colored by the grid-level change in crop raiding HEC estimates during the wet season for SSP3-RCP7.0 (top) and SSP1-RCP2.6 (bottom). Darker colors represent a greater projected increase in conflict. These are the same values provided in Table S7.

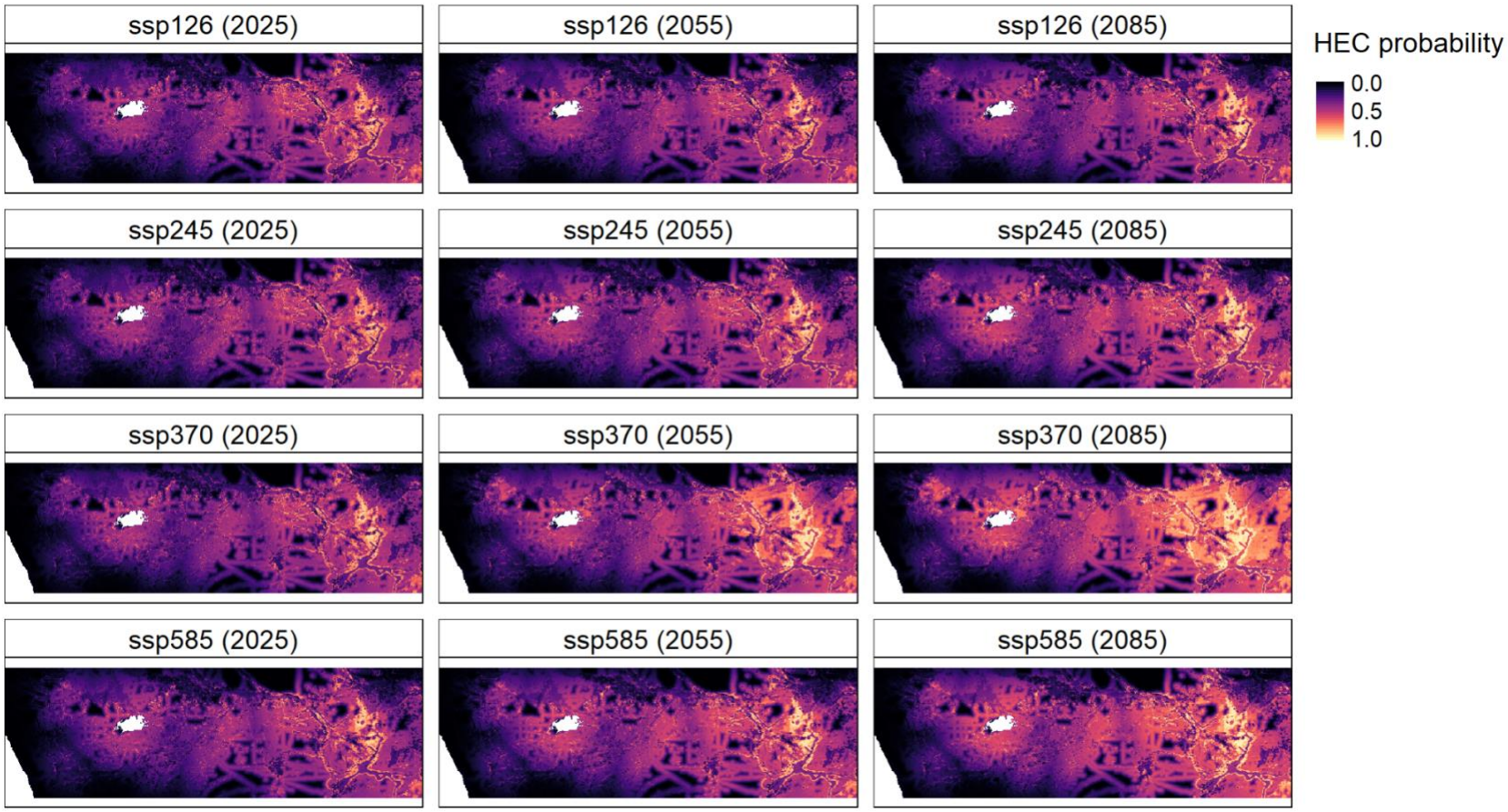

Fig. S10. Future HEC projections generated from the point process model for crop raiding conflict event probability during the dry season under four emission scenarios: SSP1-RCP2.6 ('Sustainability'), SSP2-RCP4.5 ('Middle of the Road'), SSP3-RCP7.0 ('Regional Rivalry'), and SSP5-RCP8.5 ('Fossil-Fueled Development').

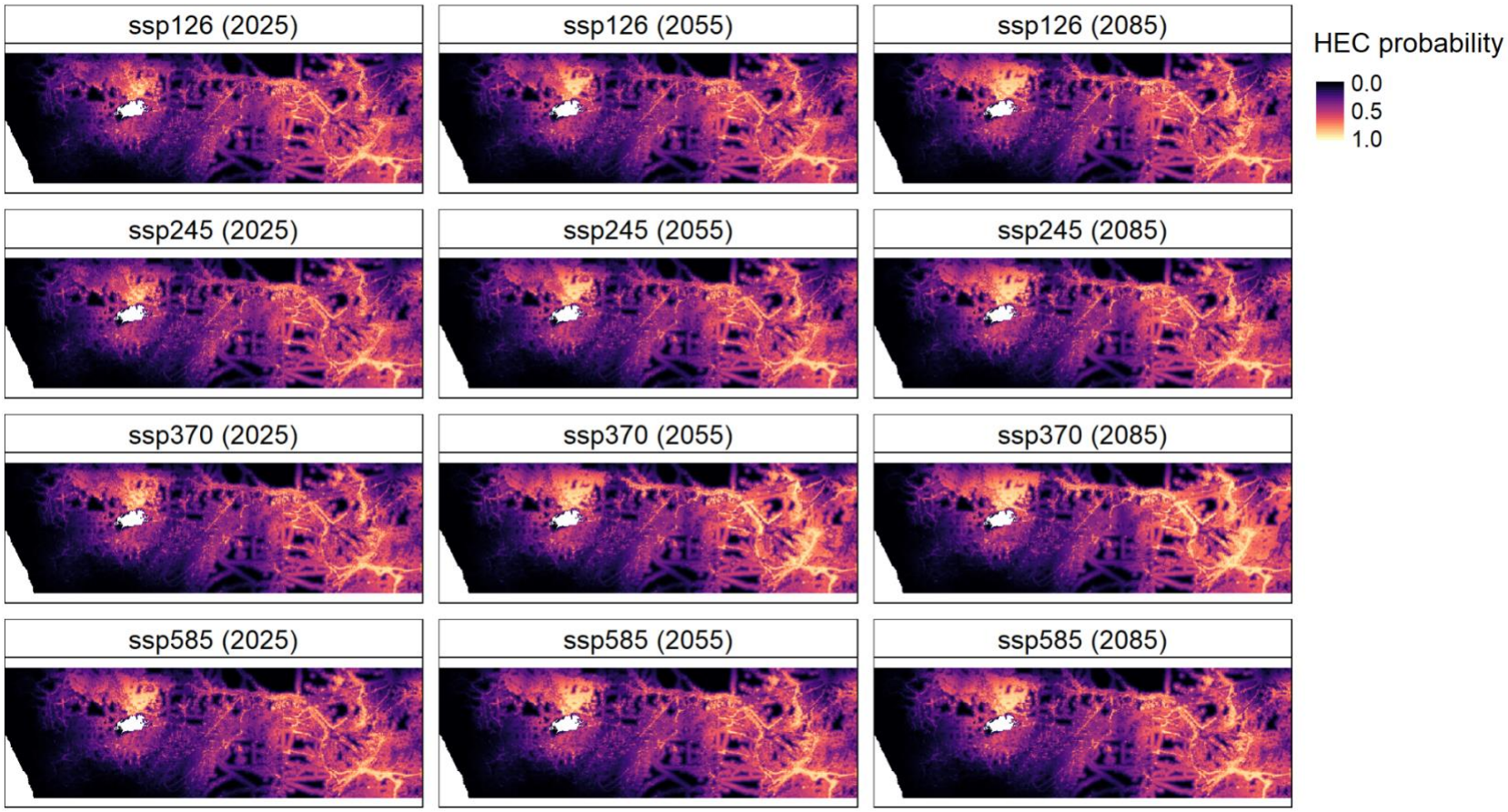

Fig. S11. Future HEC projections generated from the point process model for crop raiding conflict event probability during the wet season under four emission scenarios: SSP1-RCP2.6 ('Sustainability'), SSP2-RCP4.5 ('Middle of the Road'), SSP3-RCP7.0 ('Regional Rivalry'), and SSP5-RCP8.5 ('Fossil-Fueled Development').

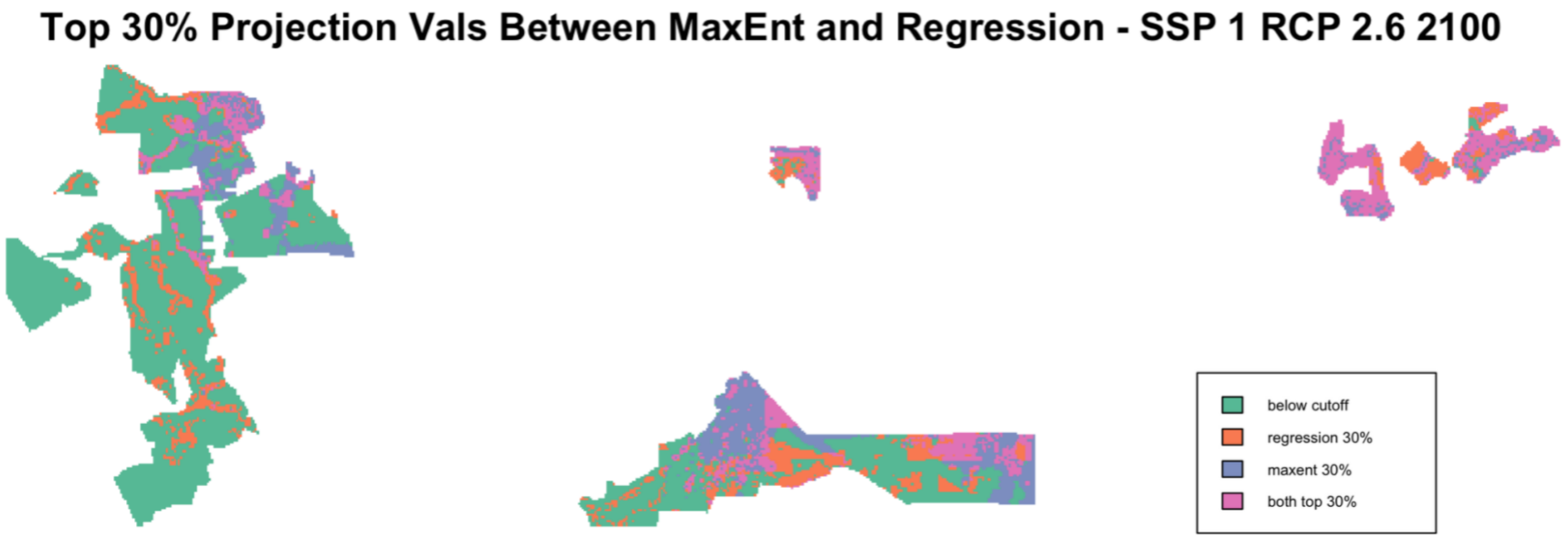

Fig. S12: Comparison of the top 30% of projected change pixels between 2025 and 2085 under both the regression and point process models for SSP1-RCP2.6. While there is some consistency between the models, regression outputs showed more linear features in Western Namibia.

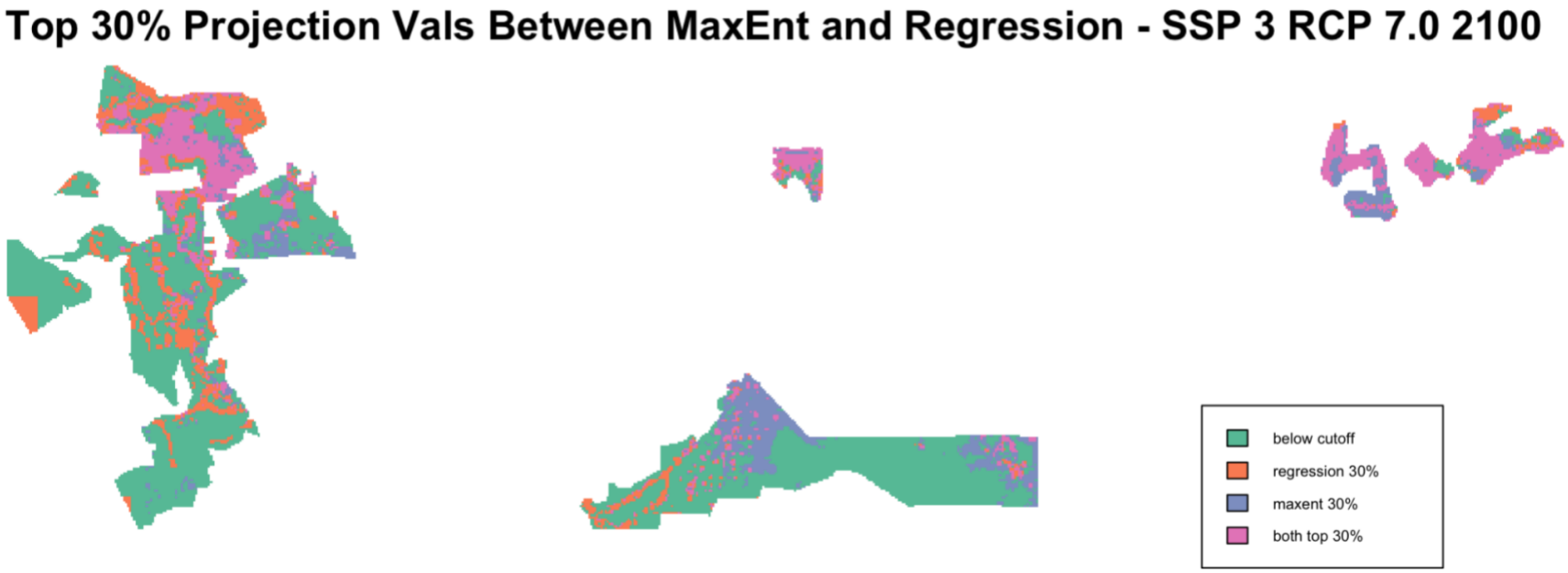

Fig. S13. Comparison of the top 30% of projected change pixels between 2025 and 2085 under both the regression and point process models for SSP3-RCP7.0. We see a larger overlap in Northwestern Namibia, as population and crop cover are expected to significantly expand there under this model.

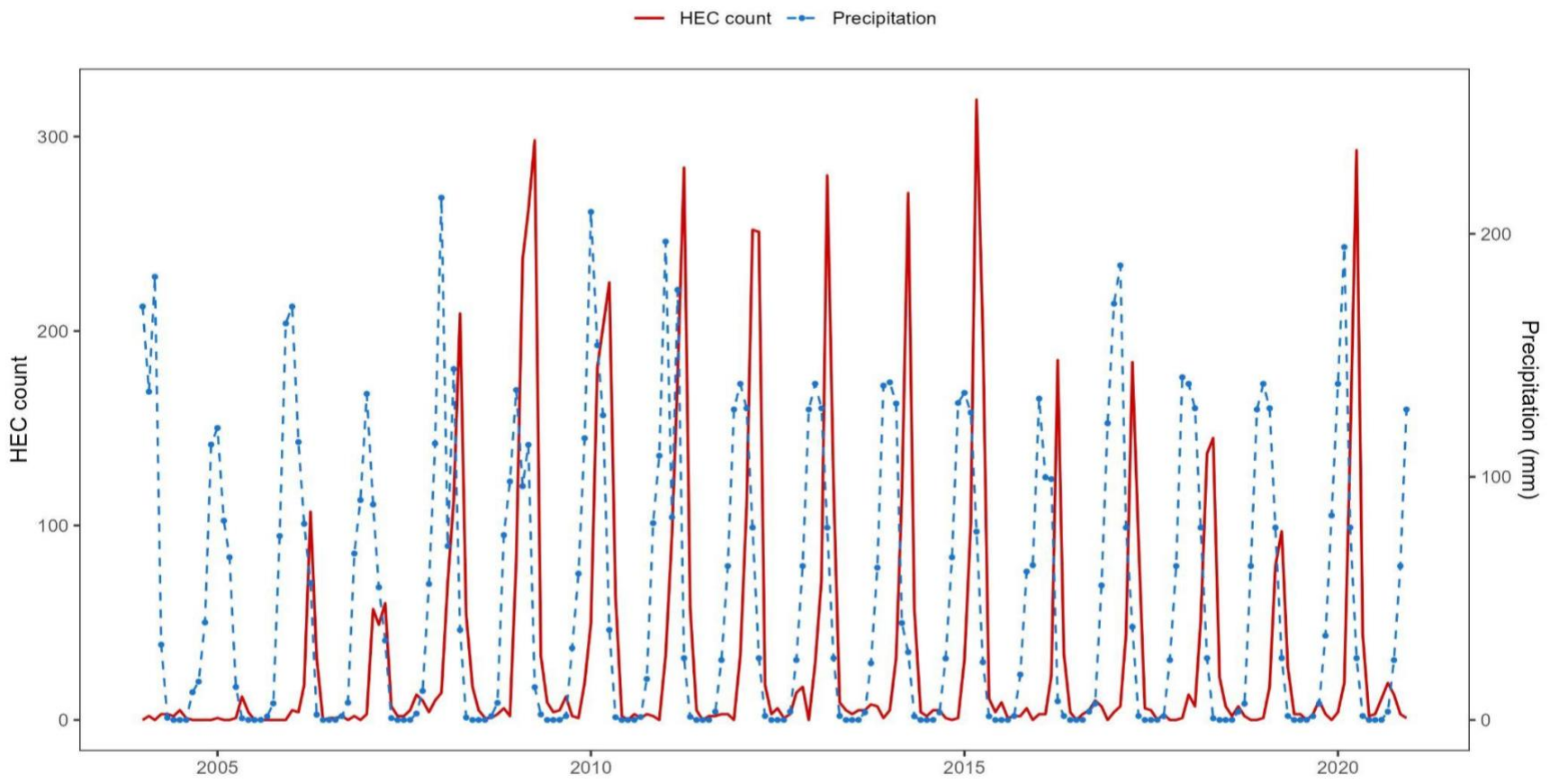

Fig. S14. HEC and mean monthly precipitation (mm) in the Zambezi Region between 2004 and 2020. HEC counts are aggregated monthly across the 15 registered communal conservancies in the Zambezi region, with mean monthly precipitation values shown by the blue dots. Precipitation data was sourced from WorldClim 2.1. Spikes in conflict following the wet season were smaller between 2004 and 2008 because not all registered communal conservancies were reporting conflict during this time, as shown in Table S9.

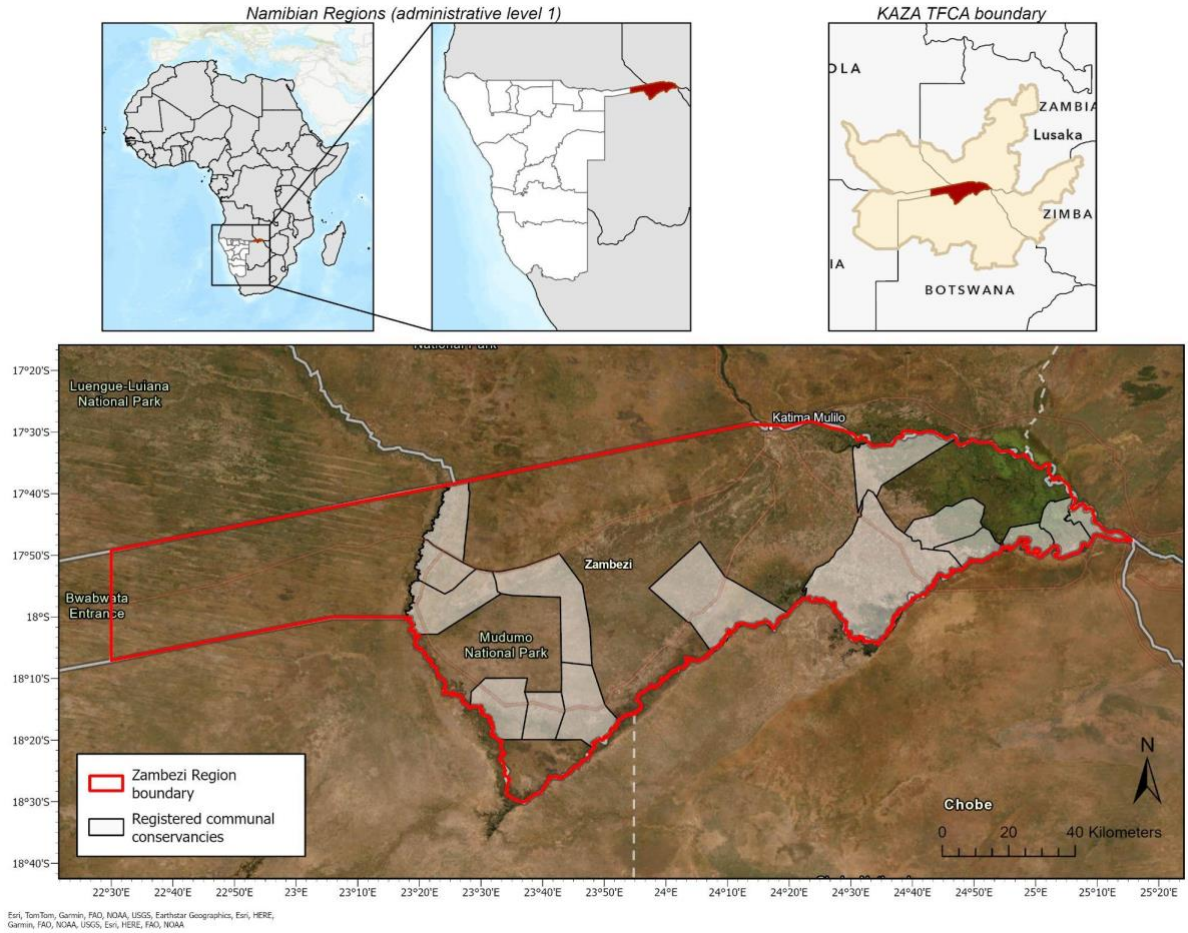

Fig. S15. Zambezi Region of Namibia with Namibian administrative level 1 regions (top left), the Kavango Zambezi Transfrontier Conservation Area (KAZA) boundary (top right), and all 15 registered communal conservancies within the Region's boundary (bottom).

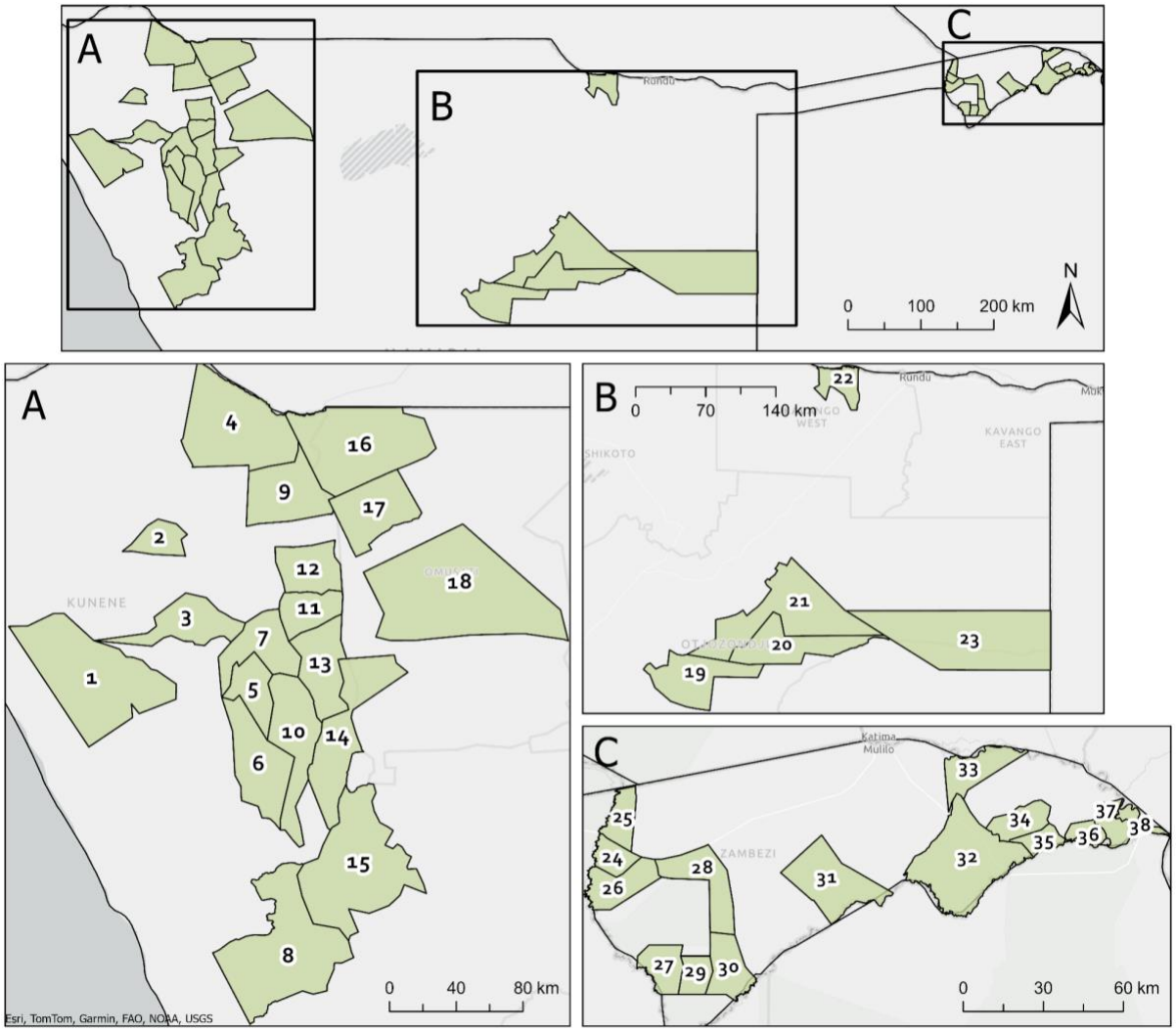

Fig. S16. All HEC reporting communal conservancies where the HEC data were collected. Insets and numbers for each conservancy in western (A), middle (B), and eastern (C) northern Namibia, and the names of each conservancy are listed in Table S10 below.

852

Season	Measure	Crop Raiding Incidents
Wet	Range:	0 - 75
	Mean:	0.06759
Dry	Range:	0 - 28
	Mean:	0.00532

853 **Table S1**. Range and mean of conflict counts per grid cell across the whole study area, split by
854 season.

Scaled Covariate	Crop Raiding	
	Wet Season	**Dry Season**
Grid spei3	0.133 (0.220)	-0.283 (0.178)
50km spei3	0.042 (0.263)	-0.465 (0.350)
Core spei3	-0.289 (0.189)	**0.818*** **(0.356)**
Worldpop	**0.910***** **(0.010)**	**1.256***** **(0.182)**
Tree Cover	-0.014 (0.066)	-0.266 (0.138)
Cropland Cover	**0.149***** **(0.037)**	0.067 (0.105)
Built Cover	0.037 (0.022)	-0.001 (0.042)
Fixed Effects:		
Season-Year	Yes	Yes
Spatial Group	Yes	Yes
Num. Obs	54888	41128
Std. Errors	by: group & year	by: group & year

Table S2. Poisson Fixed Effects coefficients and standard errors for crop raiding models. Covariates were scaled to a consistent 0-1 range before running the regression, allowing for comparable coefficients within models. * signifies a p-value of <0.05, ** refers to <0.01, and *** denotes <0.001. Count models remove within-groups without events, leading to lower numbers of observations in these models compared to the linear models.

Scaled Covariate	Crop Raiding	
	Wet Season	**Dry Season**
Grid spei3	0.019 (0.213)	**-0.458*** **(0.197)**
50km spei3	0.285 (0.229)	-0.271 (0.492)
Core spei3	-0.265 (0.205)	0.548 (0.438)
Worldpop	**1.216***** **(0.106)**	**1.319***** **(0.159)**
Tree Cover	0.019 (0.087)	-0.101 (0.193)
Cropland Cover	**0.241***** **(0.069)**	0.172 (0.110)
Built Cover	0.096 (0.120)	0.023 (0.044)
Fixed Effects:		
Season-Year	Yes	Yes
Spatial Group	Yes	Yes
Num. Obs	54888	41128
Std. Errors	by: group & year	by: group & year

Table S3. Negative Binomial Fixed Effects coefficients and standard errors for crop raiding models. Covariates were scaled to a consistent 0-1 range before running the regression, allowing for comparable coefficients within models. * signifies a p-value of <0.05, ** refers to <0.01, and *** denotes <0.001. Count models remove within-groups without events, leading to lower numbers of observations in these models compared to the linear models.

Scaled Covariate	Wet Season[1]	Dry Season
Intercept	0.299 (0.174)	0.037 (0.031)
Grid spei3	-0.124 (0.083)	0.008 (0.007)
50km spei3	0.127 (0.192)	0.019 (0.036)
Core spei3	0.031 (0.221)	-0.028 (0.034)
Worldpop	**0.266* (0.132)**	**0.050** (0.015)**
Tree Cover	**0.356** (0.093)**	0.015 (0.009)
Cropland Cover	0.247 (0.140)	-0.006 (0.010)
Built Cover	0.016 (0.016)	0.002 (0.002)
Elevation	**-0.446* (0.193)**	-0.018 (0.035)
Slope	**-0.381* (0.172)**	-0.021 (0.025)
Aspect	**0.299* (0.093)**	-0.012 (0.010)
Distance to rivers	-0.098 (0.216)	0.021 (0.048)
Distance to roads	**0.638*** (0.158)**	**0.027* (0.009)**
Distance to core areas	-0.086 (0.171)	0.021 (0.027)
Distance to Fences	**-0.681*** (0.111)**	**-0.035* (0.013)**
Distance to water	0.000 (0.000)	**-0.000002* (0.000001)**
Cropland edge length	-0.001 (0.004)	-0.001 (0.001)
Built area edge length	**-0.023*** (0.005)**	**-0.001* (0.000)**
Forest edge length	**-0.014** (0.005)**	-0.001 (0.000)

Table S4. Random Effects outcomes and standard errors for crop raiding models. Covariates were scaled to a consistent 0-1 range before running the regression, allowing for comparable coefficients within models. * signifies a p-value of <0.05, ** refers to <0.01, and *** denotes <0.001.

[1] The wet season crop raiding random effects model failed the Hausman test, meaning that it is not appropriate for causal inference as there is unobserved variation that impacts the outcome across spatial and time groups. However, we report results here to allow for some comparison with the point process models. The dry season model passed the Hausman test.

Season	HEC Occurrences	Background Points
Dry	n = 692	n = 2757
Wet	n = 1811	n = 7233

Table S5. Number of occurrences of HEC and background points used in each point process model.

Model	SSP1-RCP 2.6 Change 2025-2085	SSP2-RCP 4.5 Change 2025-2085	SSP3-RCP 7.0 Change 2025-2085	SSP5-RCP 8.5 Change 2025-2085
Wet Szn Crop Raiding	0.431 (0.382, 0.479)	0.695 (0.631, 0.760)	1.04 (0.951, 1.13)	0.502 (0.434, 0.570)
Dry Szn Crop Raiding	0.031 (0.019, 0.042)	0.048 (0.032, 0.064)	0.073 (0.051, 0.095)	0.029 (0.011, 0.047)

Table S6. Yearly change in crop raiding estimated from the fixed effects models, with a 95% CI interval calculated from a linear combination of errors in parentheses below. Scenarios are SSP1-RCP2.6 ('Sustainability'), SSP2-RCP4.5 ('Middle of the Road'), SSP3-RCP7.0 ('Regional Rivalry'), and SSP5-RCP8.5 ('Fossil-Fueled Development'). 'Fossil-Fueled Development' reports relatively low levels of land conversion and moderate population growth in the region despite high levels of emissions/warming, leading to a lower increase in HEC than other high-emissions scenarios.

887

Conservancy Name	Projected Wet Season Crop Raiding Change 2025-2085			
	SSP1-RCP2.6	SSP2-RCP4.5	SSP3-RCP7.0	SSP5-RCP8.5
≠Khoadi-//Hôas	0.448 (0.020)	0.614 (0.029)	0.757 (0.037)	0.533 (0.035)
Anabeb	0.236 (0.011)	0.317 (0.019)	0.385 (0.025)	0.319 (0.027)
Balyerwa	0.541 (0.030)	1.184 (0.046)	1.469 (0.066)	0.637 (0.034)
Bamunu	0.702 (0.039)	1.228 (0.051)	1.968 (0.075)	0.771 (0.045)
Dzoti	0.525 (0.034)	1.060 (0.042)	1.625 (0.061)	0.603 (0.040)
Ehi-Rovipuka	0.450 (0.018)	0.568 (0.026)	0.704 (0.033)	0.540 (0.030)
Impalila	9.923 (0.385)	12.787 (0.483)	21.996 (0.769)	9.645 (0.376)
Kabulabula	1.108 (0.043)	1.285 (0.048)	1.614 (0.058)	1.080 (0.045)
Kasika	2.896 (0.112)	3.827 (0.139)	6.200 (0.219)	2.803 (0.114)
Kunene River	0.577 (0.027)	0.795 (0.034)	1.095 (0.043)	0.658 (0.035)
Kwandu	3.381 (0.126)	4.654 (0.165)	7.714 (0.271)	3.283 (0.124)
Lusese	1.858 (0.068)	2.403 (0.087)	3.557 (0.129)	1.859 (0.072)
Mashi	1.110 (0.050)	1.827 (0.071)	2.762 (0.010)	1.209 (0.056)
Maurus Nekaro	1.222 (0.101)	2.625 (0.133)	3.512 (0.158)	1.295 (0.104)
Mayuni	3.053 (0.168)	5.630 (0.230)	9.383 (0.352)	2.714 (0.159)
Nakabolelwa	0.784 (0.032)	0.935 (0.036)	1.157 (0.044)	0.845 (0.037)
Okamatapati	0.115 (0.007)	0.170 (0.011)	0.224 (0.015)	0.188 (0.015)

Conservancy Name	Projected Wet Season Crop Raiding Change 2025-2085			
	SSP1-RCP2.6	SSP2-RCP4.5	SSP3-RCP7.0	SSP5-RCP8.5
Okangundumba	0.716 (0.029)	1.003 (0.040)	1.277 (0.051)	0.796 (0.039)
Okongoro	1.111 (0.040)	1.304 (0.049)	1.562 (0.060)	1.200 (0.049)
Omatendeka	0.374 (0.016)	0.487 (0.024)	0.624 (0.031)	0.461 (0.029)
Ombombo	0.667 (0.031)	0.927 (0.040)	1.331 (0.052)	0.748 (0.039)
Ombujokanguindi	0.278 (0.012)	0.359 (0.019)	0.446 (0.024)	0.367 (0.025)
Ondjou	0.089 (0.006)	0.140 (0.010)	0.187 (0.014)	0.159 (0.014)
Ongongo	0.082 (0.005)	0.143 (0.011)	0.181 (0.015)	0.170 (0.017)
Orupupa	0.574 (0.023)	0.702 (0.030)	0.889 (0.038)	0.663 (0.034)
Otjituuo	0.113 (0.008)	0.201 (0.013)	0.273 (0.017)	0.197 (0.016)
Otuzemba	0.373 (0.015)	0.481 (0.022)	0.610 (0.028)	0.464 (0.025)
Ozonahi	-0.276 (0.021)	0.059 (0.018)	0.237 (0.020)	-0.205 (0.029)
Ozondundu	0.388 (0.016)	0.492 (0.023)	0.614 (0.030)	0.477 (0.029)
Puros	0.046 (0.005)	0.094 (0.013)	0.129 (0.020)	0.138 (0.025)
Salambala	2.417 (0.105)	3.643 (0.139)	4.958 (0.181)	2.474 (0.109)
Sheya Shuushona	0.310 (0.020)	0.465 (0.025)	0.626 (0.030)	0.389 (0.030)
Sikunga	3.861 (0.161)	5.534 (0.203)	11.680 (0.410)	3.590 (0.155)
Sobbe	0.044 (0.020)	0.369 (0.023)	0.687 (0.030)	0.118 (0.026)

Conservancy Name	Projected Wet Season Crop Raiding Change 2025-2085			
	SSP1-RCP2.6	SSP2-RCP4.5	SSP3-RCP7.0	SSP5-RCP8.5
Torra	0.065 (0.008)	0.124 (0.017)	0.161 (0.023)	0.156 (0.029)
Uukolonkadhi Ruacana	0.798 (0.068)	1.821 (0.082)	3.355 (0.126)	0.832 (0.074)
Uukwaluudhi	0.194 (0.021)	0.507 (0.023)	0.659 (0.029)	0.270 (0.030)
Wuparo	0.012 (0.054)	0.342 (0.054)	1.355 (0.086)	-0.063 (0.062)

888 **Table S7.** Average HEC grid-level increases in Wet Season Crop Raiding, split by conservancy
889 and scenario. Standard errors, as derived from the Delta method (see *Materials and Methods)*,
890 are provided in parentheses beside the projected increase values.

891

Conservancy Name	Projected Dry Season Crop Raiding Change 2025-2085			
	SSP1-RCP2.6	SSP2-RCP4.5	SSP3-RCP7.0	SSP5-RCP8.5
≠Khoadi-//Hôas	0.032 (0.005)	0.042 (0.008)	0.051 (0.009)	0.033 (0.009)
Anabeb	0.016 (0.004)	0.019 (0.006)	0.023 (0.007)	0.016 (0.008)
Balyerwa	0.038 (0.007)	0.086 (0.010)	0.107 (0.014)	0.040 (0.009)
Bamunu	0.051 (0.008)	0.089 (0.011)	0.146 (0.016)	0.050 (0.011)
Dzoti	0.037 (0.007)	0.076 (0.009)	0.119 (0.013)	0.037 (0.010)
Ehi-Rovipuka	0.033 (0.005)	0.039 (0.007)	0.048 (0.009)	0.033 (0.009)
Impalila	0.765 (0.071)	0.985 (0.089)	1.697 (0.141)	0.737 (0.069)
Kabulabula	0.082 (0.008)	0.094 (0.010)	0.118 (0.012)	0.074 (0.010)
Kasika	0.221 (0.021)	0.291 (0.027)	0.473 (0.041)	0.207 (0.023)
Kunene River	0.042 (0.007)	0.056 (0.009)	0.077 (0.011)	0.041 (0.010)
Kwandu	0.258 (0.023)	0.354 (0.031)	0.591 (0.050)	0.245 (0.024)
Lusese	0.140 (0.013)	0.180 (0.018)	0.268 (0.025)	0.134 (0.015)
Mashi	0.082 (0.010)	0.135 (0.014)	0.208 (0.020)	0.084 (0.012)
Maurus Nekaro	0.091 (0.019)	0.197 (0.026)	0.264 (0.031)	0.090 (0.021)
Mayuni	0.232 (0.031)	0.429 (0.043)	0.720 (0.065)	0.201 (0.030)
Nakabolelwa	0.057 (0.007)	0.067 (0.008)	0.082 (0.010)	0.056 (0.009)
Okamatapati	0.006 (0.003)	0.007 (0.005)	0.009 (0.006)	0.004 (0.006)

Conservancy Name	Projected Dry Season Crop Raiding Change 2025-2085			
	SSP1-RCP2.6	SSP2-RCP4.5	SSP3-RCP7.0	SSP5-RCP8.5
Okangundumba	0.053 (0.007)	0.072 (0.010)	0.092 (0.012)	0.053 (0.010)
Okongoro	0.084 (0.009)	0.095 (0.011)	0.114 (0.014)	0.084 (0.012)
Omatendeka	0.027 (0.005)	0.032 (0.007)	0.041 (0.009)	0.027 (0.008)
Ombombo	0.049 (0.007)	0.066 (0.010)	0.096 (0.012)	0.048 (0.010)
Ombujokanguindi	0.019 (0.004)	0.022 (0.006)	0.028 (0.008)	0.020 (0.008)
Ondjou	0.004 (0.003)	0.005 (0.004)	0.007 (0.006)	0.003 (0.006)
Ongongo	0.004 (0.003)	0.006 (0.005)	0.007 (0.006)	0.004 (0.007)
Orupupa	0.042 (0.006)	0.049 (0.008)	0.062 (0.010)	0.043 (0.009)
Otjituuo	0.006 (0.003)	0.009 (0.005)	0.013 (0.007)	0.005 (0.007)
Otuzemba	0.027 (0.005)	0.032 (0.007)	0.040 (0.009)	0.027 (0.008)
Ozonahi	-0.024 (0.005)	-0.002 (0.006)	0.010 (0.007)	-0.027 (0.009)
Ozondundu	0.028 (0.005)	0.033 (0.007)	0.041 (0.009)	0.029 (0.008)
Puros	0.001 (0.003)	0.001 (0.005)	0.002 (0.006)	0.002 (0.007)
Salambala	0.184 (0.020)	0.276 (0.026)	0.377 (0.034)	0.182 (0.021)
Sheya Shuushona	0.021 (0.006)	0.030 (0.007)	0.040 (0.009)	0.020 (0.009)
Sikunga	0.295 (0.030)	0.423 (0.038)	0.898 (0.076)	0.268 (0.030)
Sobbe	-0.001 (0.005)	0.022 (0.006)	0.047 (0.008)	0.000 (0.007)

Conservancy Name	Projected Dry Season Crop Raiding Change 2025-2085			
	SSP1-RCP2.6	SSP2-RCP4.5	SSP3-RCP7.0	SSP5-RCP8.5
Torra	0.002 (0.003)	0.004 (0.005)	0.005 (0.006)	0.003 (0.007)
Uukolonkadhi Ruacana	0.059 (0.013)	0.135 (0.017)	0.251 (0.025)	0.054 (0.016)
Uukwaluudhi	0.012 (0.006)	0.033 (0.007)	0.043 (0.009)	0.011 (0.009)
Wuparo	-0.003 (0.011)	0.021 (0.012)	0.099 (0.018)	-0.014 (0.014)

892 **Table S8.** Average HEC grid-level increases in Dry Season Crop Raiding, split by conservancy and
893 scenario. Standard errors, as derived from the Delta method (see *Materials and Methods)*, are
894 provided in parentheses beside the projected increase values.

Conservancy Name	Year of Registry	Area (km.)	Region	Reporting Date	Population Size
≠Khoadi-//Hôas	1998	3353.08	Kunene	2/7/2007	5629
Anabeb	2003	1569.99	Kunene	2/12/2016	1562
Balyerwa	2006	225.20	Zambezi	1/20/2006	1462
Bamunu	2011	555.92	Zambezi	1/12/2009	2302
Dzoti	2009	287.00	Zambezi	1/9/2009	2286
Ehi-Rovipuka	2001	1979.81	Kunene	9/6/2010	1346
Impalila	2005	72.50	Zambezi	1/30/2006	1000
Kabulabula	2011	89.00	Zambezi	2/3/2009	421
Kasika	2005	146.59	Zambezi	4/16/2009	1085
Kunene River	2006	2763.61	Kunene	1/31/2018	8499
Kwandu	1999	189.52	Zambezi	1/8/2008	4005
Lusese	2014	206.50	Zambezi	2/5/2010	1340
Mashi	2003	296.77	Zambezi	5/19/2004	2523
Maurus Nekaro	2017	1117.41	Kavango	3/5/2018	13328
Mayuni	1999	150.57	Zambezi	2/15/2004	2759
Nakabolelwa	2014	114.00	Zambezi	5/7/2005	842

Conservancy Name	Year of Registry	Area (km.)	Region	Reporting Date	Population Size
Okamatapati	2005	3095.57	Otjozondjupa	12/14/2018	2066
Okangundumba	2003	1130.75	Kunene	1/3/2007	2331
Okongoro	2012	956.00	Kunene	1/27/2016	2230
Omatendeka	2003	1619.38	Kunene	2/6/2007	2939
Ombombo	2014	1486.76	Kunene	2/9/2016	3180
Ombujokanguindi	2012	1160.00	Kunene	6/1/2018	652
Ondjou	2006	8729.00	Omaheke	1/29/2019	3068
Ongongo	2012	501.32	Kunene	4/6/2016	971
Orupupa	2011	1234.14	Kunene	3/5/2007	1387
Otjituuo	2005	6132.52	Otjozondjupa	4/20/2020	5971
Otuzemba	2012	741.76	Kunene	5/2/2007	449
Ozonahi	2005	3203.53	Otjozondjupa	2/7/2021	11614
Ozondundu	2003	745.35	Kunene	9/22/2007	390
Puros	2000	3562.43	Kunene	5/1/2017	1584
Salambala	1998	929.79	Zambezi	1/30/2007	9193
Sheya Shuushona	2005	5065.57	Omusati	2/21/2016	3789
Sikunga	2009	286.70	Zambezi	4/15/2007	2478

Conservancy Name	Year of Registry	Area (km.)	Region	Reporting Date	Population Size
Sobbe	2006	390.70	Zambezi	1/11/2009	1115
Torra	1998	3492.76	Kunene	1/24/2011	1520
Uukolonkadhi Ruacana	2005	2992.91	Omusati	2/16/2016	37712
Uukwaluudhi	2003	1436.78	Omusati	4/10/2016	1088
Wuparo	1999	147.6	Zambezi	2/14/2006	987

898 **Table S9**. Summary data of conservancies from NASCO

899

Number in SI Appendix Fig. E4	Conservancy
Puros	1
Ongongo	2
Ombujokanguindi	3
Kunene River	4
Ozondundu	5
Anabeb	6
Okangundumba	7
Torra	8
Ombombo	9
Omatendeka	10
Otuzemba	11
Okongoro	12
Orupupa	13
Ehi-Rovipuka	14
≠Khoadi-//Hôas	15
Uukolonkadhi Ruacana	16
Uukwaluudhi	17
Sheya Shuushona	18
Ozonahi	19
Okamatapati	20
Otjituuo	21
Maurus Nekaro	22
Ondjou	23
Mayuni	24
Kwandu	25
Mashi	26
Balyerwa	27
Sobbe	28
Wuparo	29
Dzoti	30
Bamunu	31
Salambala	32
Sikunga	33
Lusese	34

Number in SI Appendix Fig. E4	Conservancy
Nakabolelwa	35
Kabulabula	36
Kasika	37
Impalila	38

900 **Table S10.** HEC reporting communal conservancies associated with Figure S16.